

# The IRM Quarterly

Winter 2019-2020, Vol. 29 No.4

Inside...

Visiting Fellows Reports	2
Current Articles	10
New Visiting Fellows	9

## Foundations of Magnetic Anisotropy: A Brief Review

Mike Jackson, IRM

The earliest descriptions of magnetic anisotropy that I'm aware of appear in William Gilbert's book *On the Magnet*, published more than 4 centuries ago. Although he doesn't actually use the word "anisotropy", which didn't exist until the mid 19th century, there are relevant ideas that come through clearly in his writing.

For example, here is a passage describing the anisotropic acquisition of thermoremanence (Fig. 1): "Let the blacksmith beat out upon his anvil a glowing mass of iron ... into an iron spike.... Let the smith be standing with his face to the north..., so that the hot iron on being struck has a motion of extension to the north. ...it is demonstrable that all those which are thus beaten out ... and so placed whilst they are cooling, turn about on their centres..., the determined end being toward the north..." What he means by 'turning about on their centers' is that, if such a spike is mounted on a suitable pivot, or set to float on a piece of wood in water, it will act as a magnetic compass needle, spontaneously returning to the orientation that it had while cooling, because of a strong and stable TRM component along its long axis. "Those, however, which are pointed or drawn out rather toward the eastern or western point, conceive hardly any verticity or a very undecided one." In other words, if they cool with the field along their short axes they acquire only a weak TRM and don't have a strong tendency to orient in any particular direction in the Earth's field.

In another passage he describes the magnetic intensity of lodestones as it relates to their shapes: "... a slightly longer stone attracts more than a spherical one... even if the stones are both from the same mine and of the same weight and size". Before I get to Gilbert's explanation of this interesting observation, let me quickly refresh your memory about the modern textbook explanation of shape anisotropy for comparison.

Figure 2 shows an ellipsoidal particle, uniformly magnetized along its long and short dimensions. Where the magnetization terminates at the surface of the grain, it can be imagined to result in the formation of magnetic poles or magnetostatic charges, which are the sources of the external  $H$  field and of the internal demagnetizing field. When the particle is magnetized along its long dimension, there is a relatively small fraction of the surface covered



Fig. 1. A thermoremanent anisotropy experiment described by William Gilbert in 1600. When a red-hot iron spike is allowed to cool while pointing from the south (Auster) to the north (Septentrio), it acquires a strong remanence. Cooling in the east-west orientation, with the long axis perpendicular to the ambient field, produces a much weaker TRM.

with poles, and a relatively large separation of the + and - charges, so the magnetostatic potential gradient is shallow and the demagnetizing field is weak. In contrast when  $M$  is along the short dimension, a larger fraction of the grain surface is covered with poles, and the separation between + and - poles is small, so the demagnetizing field is strong; this orientation is energetically unfavorable for the magnetization.

Now here's how Gilbert explains it: "The way from pole to pole is longer in a longer stone, and the forces brought together from other parts are not so scattered as in a round magnet.... A much weaker office, however, does a plane or oblong stone perform, when ... the pole ... is spread over the flat... so that it is esteemed as one of an abject and contemptible class, according to its less apt and less suitable figure." The idea is clear: whatever natural process has magnetized the lodestones, it has operated more effectively along the long dimension of the stones.



William Gilbert  
1544-1603

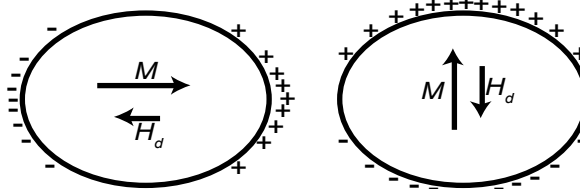


Fig. 2. Shape anisotropy derives from the fictitious magnetostatic poles that form at the discontinuity between a magnetic material (with magnetization  $M$ ) and its surrounding nonmagnetic medium, which give rise to the demagnetizing field  $H_d$ . Both  $M$  and  $H_d$  are uniform within the ellipsoidal grain shown (after Dunlop & Özdemir, 1997).

cont'd. on  
pg. 14...

# Visiting Fellow's Reports

## Disentangling the timing of chemical remagnetizations in carbonates. Case of the Central High Atlas basin (Morocco)

P. Calvin and J.J. Villalain  
Universidad de Burgos, Spain  
pcalvin@ubu.es

### Introduction

Widespread chemical remagnetizations affecting sedimentary rocks are common processes in intraplate basins that reached a minimum of burial (i.e. few kilometers). This process consists in the neoformation of ferromagnetic *s.l.* minerals, generally magnetite and pyrrhotite in carbonates and black-shales and pigmentary hematite in red-beds, related (among other factors) with the increase of the temperature (e.g. Van der Voo and Torsvik et al., 2012, and references therein). Here in particular, we show rock magnetic results from Jurassic carbonates from the Central High Atlas basin (Morocco).

These rocks show a homogeneous paleomagnetic behavior, with unblocking temperatures for the viscous paleomagnetic component up to 200-250°C and for the characteristic paleomagnetic component between 250 and 450-500 °C. Both are carried by authigenic uniaxial SSD magnetite (with differences in grain size) formed during the remagnetization process (Calvin et al., 2018). The characteristic paleomagnetic component shows systematically normal polarity and the calculated mean remagnetization direction plots on the apparent polar wander path at ca. 100 Ma (Torres-López et al., 2014). Following this observation, the age of this remagnetization has been assumed as ca. 100 Ma, i.e. during the Cretaceous Normal Superchron (CNS). However, if an increase of temperature related with burial was the trigger of the neoformation of the magnetite grains, they could have started to grow and to block their magnetic moments from the Middle-Upper Jurassic up to the inversion of the basin during the Cenozoic.

In view of these considerations, one of the main challenges studying chemical remagnetizations is to assess the timing under which these processes happened, i.e. short vs. long remagnetization periods. Then, we ask ourselves, is the remagnetization of the Central High Atlas just a punctuated process that happened around 100 Ma? Alternatively, is the ca. 100 Ma paleomagnetic direction just the average of magnetic moments of the entire SSD magnetite population that grew from the Middle Jurassic up to the Cenozoic? This question has its validity since the apparent polar wander path of Africa for this time

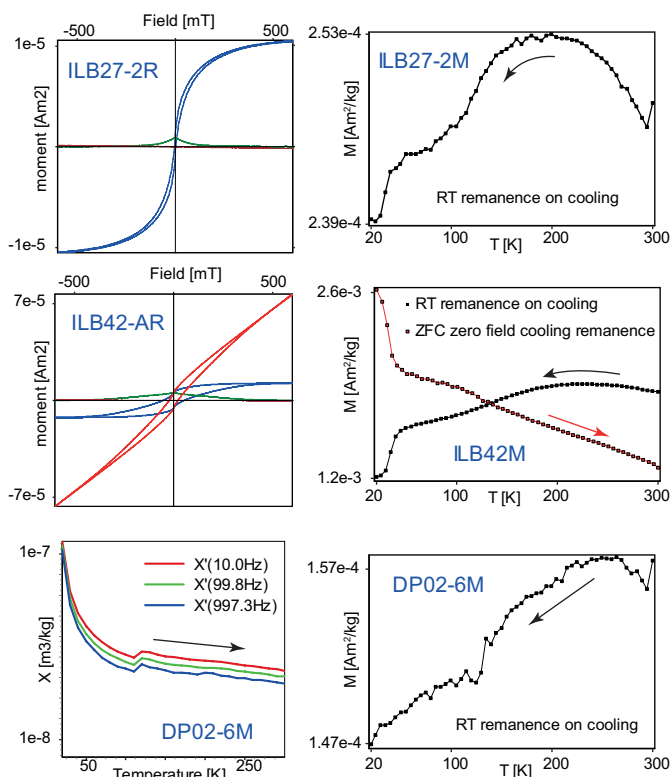


Fig. 1: Hysteresis loops and low temperature curves showing different magnetic behaviors.

(Torsvik et al., 2012) shows, in the study area, a progressive rotation without latitude change, and the CNS (and also the ca. 100 Ma age) is just in the middle of this time. Therefore, it is possible to imagine a model in which a constant and progressive growth and blocking of SSD authigenic magnetite grains records 'normal and reverse magnetic moments' and whose average was the CNS paleomagnetic direction.

We try to assess the effectiveness of the SSD grains carrying the remagnetization to answer these questions; we compare the NRM and the ARM signal through the pseudo-Thellier approach (Tauxe et al., 1995). In this case, we use the Arai plot in order to observe differences in slope and/or behavior both at the sample scale (comparing slopes in different coercivity spectra) and between samples corresponding to different stratigraphic positions within the Jurassic sequence.

### Experiments

During the short stay at the IRM we performed some measurements in 90 samples of Lower and Middle Jurassic carbonates from the Central High Atlas. Across 23 steps from 0 to 170 mT, samples were treated according to the following work routine in the 2G u-channel magnetometer: (i) AF demagnetization of the NRM, (ii) ARM acquisition using a constant DC field of 50  $\mu$ T and (iii) AF demagnetization of the ARM.

Additionally, several rock magnetic experiments were performed to monitor possible differences in rock magnetic properties between samples. VSMs (Princeton Measurements) were used to measure hysteresis loops, backfield curves and FORC diagrams. Low temperature curves of remanence (RTSIRM and ZFC) and susceptibility were measured in the MPMS (Quantum Design).

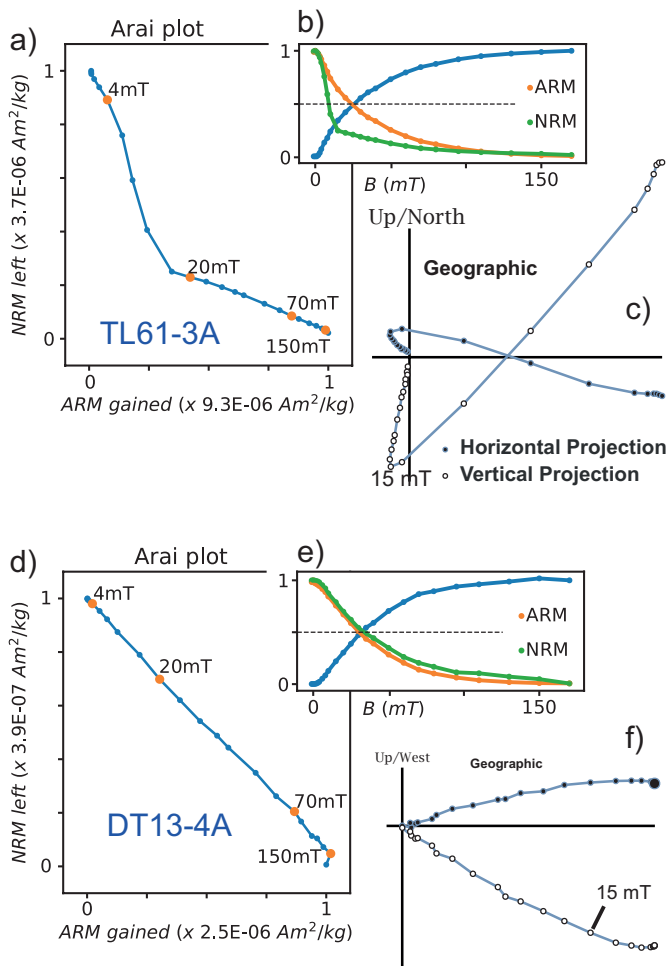


Fig. 2. The two end-member behavior: a,d) Arai plots; b,e) increment/decay of magnetization during ARM acquisition/AF demagnetization of NRM and ARM; c,f) orthogonal plot of the AF demagnetization of NRM.

## Results

Rock magnetic experiments (Fig. 1) show variable proportions of magnetite and pyrrhotite along the measured samples. This generates wasp-waisted hysteresis loops as a consequence of the presence of phases with different coercivity, i.e. SP and SSD magnetite and pyrrhotite. Remanence cooling curves show either the Verwey and Besnus magnetic transitions (characteristic of magnetite and pyrrhotite respectively) or both, and susceptibility curves are highly frequency-dependent, as expected for both pyrrhotite and magnetite nano-particles. This behavior is typical of chemically remagnetized rocks.

Without considering outliers, Arai plots show two end-member behaviors (Fig. 2). TL61 sample shows well differentiated curve-sections with different slopes. The first one (4-15 mT) presents higher slope and corresponds to the viscous component in the demagnetization diagram, and the second one (20-70 mT) corresponds with SSD magnetite carrying the remagnetized component (according to thermal demagnetization of the NRM). On the other hand, some samples show straight Arai plots that seem to correlate with straight demagnetization diagrams. Both in curved as in straight (from 0 to 70 mT) Arai plots, between 70 and 150 mT the slope is similar or greater than in the previous interval, and some samples are not fully demagnetized at 150 mT. We interpret this due to

the presence of a mix between magnetite and pyrrhotite (70-150mT) or only pyrrhotite (>150m T). In the following we only consider the interval between 0 and 70 mT, trying to exclude the pyrrhotite from the interpretations.

Those shown in the figure are end-members (for the 0-70 mT interval) and different developments of the viscous component are observed along the studied samples. In the same way, this viscous component observed in the NRM can correlate either with the present-day geomagnetic field or with random directions probably acquired in the laboratory. Although the viscous component, when it is present, usually extends from 0 to 20 mT, it can appear up to higher fields and seems to correlate with the change in slope in the Arai plot. The possible correlation between changes in slopes with the viscous and the characteristic component could indicate a greater effectiveness at carrying the remanence of the viscous rather than the stable population of magnetite grains (with longer relaxation times). Considering that all magnetite grains have similar characteristics and their stability only depends on their size, the less effectiveness of stable grains can be due to a distribution of grains in normal and inverse polarity groups, pointing to the long-remagnetization model. Additionally, we performed a rude correlation of slopes (20-70 mT) from the different samples that do not show any correlation with either age and/or sampling locality. In any case, more detailed treatments of the results are necessary for the moment in order to solve the posed questions.

## Acknowledgment

Special thanks to Mike Jackson, Dario Bilardello and Peter Solheid for their assistance during our stay at the IRM, as well as the IRM and the Spanish Ministry of Economy and Competitiveness (CGL2016-77560 project) for the economic support.

## References

- Calvín, P., Villalain, J.J., Casas-Sainz, A.M., 2018. Anisotropic magnetite growth in remagnetized limestones: Tectonic constraints and implications for basin history. *Geology* 46, 751–754.
- Tauxe, L., Pick, T., Kok, Y.S., 1995. Relative paleointensity in sediments: A Pseudo-Thellier Approach. *Geophysical Research Letters* 22, 2885–2888.
- Torres-López, S., Villalain, J.J.J., Casas, A.M.M., EL Ouardi, H., Moussaid, B., Ruiz-Martínez, V.C.C., 2014. Widespread Cretaceous secondary magnetization in the High Atlas (Morocco). A common origin for the Cretaceous remagnetizations in the western Tethys? *Journal of the Geological Society* 171, 673–687.
- Torsvik, T.H., Van der Voo, R., Preeden, U., Mac Niocail, C., Steinberger, B., Doubrovine, P. V., van Hinsbergen, D.J.J., Domeier, M., Gaina, C., Tohver, E., Meert, J.G., McCausland, P.J.A., Cocks, L.R.M., 2012. Phanerozoic polar wander, palaeogeography and dynamics. *Earth-Science Reviews* 114, 325–368.
- Van Der Voo, R., Torsvik, T.H., 2012. The history of remagnetization of sedimentary rocks: deceptions, developments and discoveries. *Geological Society, London, Special Publications* 371, 23–53.

## Magnetic fatigue

Boris Reznik

Karlsruhe Institute of Technology, Germany

boris.reznik@kit.edu

It is experimentally shown that cyclic or fatigue loading may deteriorate the strength of rocks under conditions, where the nominal maximum stress values responsible for rock damage are much lower than the rock strength limit (Liang et al. 2012). In nature, rock fatigue can be triggered by seismic waves leading to earthquake propagation or volcano eruption. Therefore, to gain an insight into fatigue mechanisms, investigations of amplitude- and frequency-dependent fatigue loading on the physical properties of rocks are of fundamental importance. However, no studies are known to show a magnetic response to seismic-related fatigue loading. The aim of this study is to test whether rock magnetic properties are sensitive to cyclic loading in the form of magnetic fatigue (MF) of magnetite.

For the magnetic measurements conducted at IRM, samples of a metamorphic quartz-magnetite banded iron ore described in detail elsewhere (Reznik et al. 2016) were cyclically compressed by an Instron Universal Testing Machine with 0.1 Hz. The first set of compression experiments was carried out during 1800 cycles at ambient conditions under 500°C using static stress of 70 MPa and a modulated stress of 40 MPa. In these samples, using reflected light microscopy, we observed about 1  $\mu\text{m}$  thick lamellae of hematite along grain boundaries of magnetite. To eliminate the effect of oxidation on MF, the second set of experiments was carried out at 500°C but under controlled vacuum conditions. In this case, the static stress of 150 MPa was modulated with 30 MPa during 10000 cycles. Using room temperature hysteresis measurements and low-temperature magnetometry, the following samples were comparatively studied: a sample from the initial Norway ore (Nch sample), a sample compressed static at 500°C in air (N500C sample), a sample cyclic loaded at 500°C in air (N500CL sample) and a sample cyclic loaded at 500°C in vacuum (NCLV sample).

Figure 1 presents hysteresis behavior measured by a Princeton Measurements vibrating sample magnetometer (VSM). Figure 1a is a Day plot showing that compared to the initial MD magnetite (sample Nch), the remanence ratios of fatigued samples are slightly shifted towards the PSD field. This behavior suggests a refinement of magnetic domains. The positions of the oxidized samples N500C and N500CL lie close to those of the unoxidized Nch and NCLV samples, i.e. the presence of hematite cannot be definitely deduced from the Day plot (Fig. 1a). At the same time, remanence coercivity (Bcr) and remanent magnetization (Mr) are more sensitive to the loading prehistory (Fig. 1b). Compared to the initial ore, Mr of the oxidized N500C sample is lower. This behavior can be related to magnetite oxidation while the Mr increase in the fatigued samples N500CL and NCLV can be ascribed to

the increasing MF effect (Fig. 1b, red symbols). Similarly, the increase of  $B_{cr}$  in sample N500C can be attributed to partial magnetite oxidation, while its followed drop manifests again the MF effect. Note this effect is especially developed in the case of the NCLV sample, which was subjected to relatively high, 150 MPa loading. The coercivity distributions derived from backfield remanence data suggests that the MF corresponds to a refinement of magnetic domains (Figs. 1c,d). Interestingly, the coercivity (Fig. 1d) lies near to coercivity values reported for pedogenic magnetite exhibiting magnetic behavior of superparamagnetic (<30 nm) or single domain (30-75 nm) grains (Maxbauer et al. 2017). The trend in coercivity values (Fig. 1d) is in good accordance with the Day plot behavior suggesting refinement of magnetic domains in

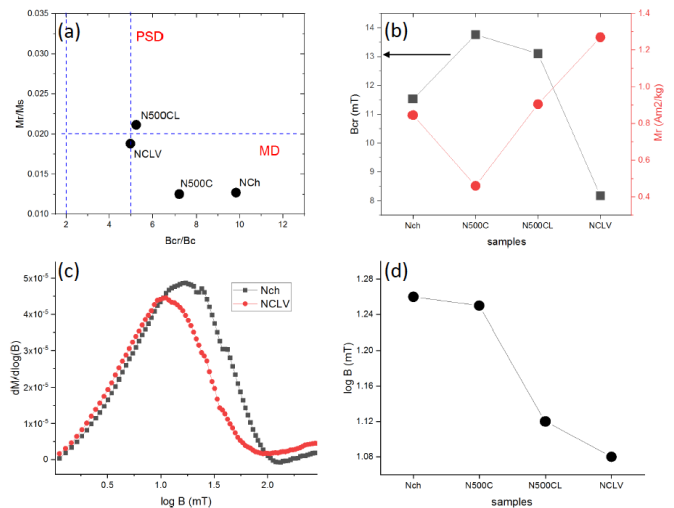


Fig. 2. Effect of loading conditions on hysteresis parameters. (a) Day plot; (b) Evolution of coercivity,  $B_{cr}$  (quadrats), and remanence,  $M_r$  (circles), values; (c) Example showing coercivity curves for Nch (black) and NCLV (red) samples; (d) Evolution of  $\log B$  values.

fatigued samples (Fig. 1a).

Figure 2 illustrates magnetic properties extracted from low-temperature measurements using a Magnetic Property Measurement System (MPMS). Saturation isothermal remanent magnetization at room temperature (RTSIRM) was produced in a magnetic field of 2.5 T at 300 K. After saturation in the imparted field, the sample NCLV exhibits the highest remanence value (Fig. 2a). This behavior is in good accordance with the hysteresis behavior measured by VSM (Fig. 1b) and proves the onset of MF in the form of single-domain grains. Some features of the loading prehistory of samples can be studied from the evolution of the p-ratio (Fig. 2b) where magnetization at 20 K is related to magnetization at 300 K. Compared to the initial sample Nch, the p-ratio values of the oxidized samples N500CL and N500C are distinctly lower. At the same time, compared to the oxidized samples, the p-ratio of the vacuum fatigued sample NCLV is higher and attributes to MF. During zero-field cooling (ZFC), all samples exhibit a relatively sharp Verwey transition ( $T_V$ ) close to 120 K (Fig. 2c). Using the first derivative of ZFC curves, the exact position of transition was determined (Fig. 2d). The distinct drop in  $T_V$  of oxidized samples indicates

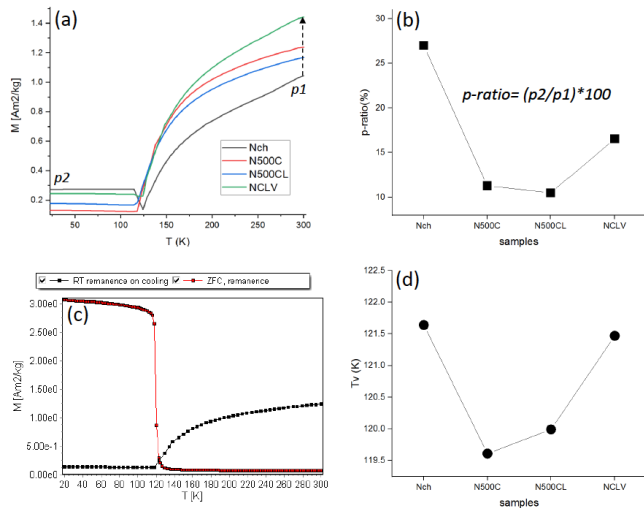


Fig. 2. Effect of loading conditions on remanence parameters. (a) RT remanence on cooling curves. The dashed arrow points to the increasing RTSIRM; (b) Variation in values of  $p$ -ratio; (c) Representative sharp RT and ZFC curves (shown for sample N500C); (d) Variation in the position of Verwey transition ( $T_V$ ).

that the transformation into hematite occurs via oxidized magnetite while the NCLV sample does not show a change in  $T_V$  compared to the initial sample.

This study demonstrates the influence of fatigue loading conditions on rock magnetic properties of a magnetite-bearing ore. In the case of loading in a vacuum, magnetic fatigue is related to the refinement of magnetic domains exhibiting increased magnetic memory. When cyclic loading occurs at ambient conditions, magnetic fatigue in magnetite is accompanied by its partial transformation into hematite. The signals related to hematite, however, cannot be easily extracted from bulk magnetic methods because they are masked by the much stronger signals of magnetite. Thus magnetic data should be validated by a microstructural sensitive method like microscopy or x-ray diffraction.

### Acknowledgments

This work was funded by DFG-Project „Magnetic fatigue“ (KO1514/13-1, SCH1545/9-1). I am grateful to Mario Walter for conducting compression tests while I am indebted to Mike Jackson for assistance with magnetic measurements.

### References

- Liang, W., Zhang, C., Gao, H., Yang, X., Xu, S. & Zhao, Y. (2012) Experiments on mechanical properties of salt rocks under cyclic loading. *J. Rock Mech. Geotech. Eng.*, 4, 54–61. doi:10.3724/SP.J.1235.2012.00054
- Maxbauer, D.P., Feinberg, J.M., Fox, D.L. & Nater, E.A. (2017) Response of pedogenic magnetite to changing vegetation in soils developed under uniform climate, topography, and parent material. *Sci. Rep.*, 7, 1–10, Springer US. doi:10.1038/s41598-017-17722-2
- Reznik, B., Kontny, A., Fritz, J. & Gerhards, U. (2016) Shock-induced deformation phenomena in magnetite and their consequences on magnetic properties. *Geochemistry, Geophys. Geosystems*, 17, 2374–2393. doi:10.1002/2016GC006338.

## Teasing out detrital and chemical remanence in hematite-bearing sedimentary rocks: insights from fluvial intraclasts

Nicholas Swanson-Hysell, UC Berkeley  
swanson-hysell@berkeley.edu

In November of 2018, just prior to the Thanksgiving holiday, I had the opportunity to visit the Institute for Rock Magnetism as a visiting fellow. This visiting fellowship was focused on furthering a study of siltstone intraclasts within particularly well-preserved fluvial sediments of the 1.1-billion-year-old Freda Formation from the North American Midcontinent Rift. As always, this visit was intellectually invigorating and involved the acquisition of high-quality data on IRM instrumentation. Peat Solheid, Mike Jackson, and Dario Bilardello were there to provide excellent technical support and advice on experimental design. Discussions with them, and with Josh Feinberg and Bruce Moskowitz, provided insight on rock magnetic data interpretation. In this visiting fellow report, I will seek to provide the main take-aways from this study which will include discussing thermal demagnetization data that were developed in the UC Berkeley Paleomagnetism lab prior to the fellowship.

As those immersed in rock magnetism are well aware, there is a long history of leveraging the magnetization of hematite-bearing sedimentary rocks to gain insight into the behavior of the ancient geomagnetic field and the paleogeographic positions of sedimentary basins. There is an accompanying long history (at times dubbed the “red bed controversy”) of seeking to constrain the age of the ancient remanence. The difficulty in doing so arises from the reality that hematite within sedimentary rocks can have two sources: (1) detrital grains that are within the sediment at the time of deposition and acquired a detrital remanent magnetization (DRM); and (2) grains that grow in situ after the sediment had been deposited and acquired a chemical remanent magnetization (CRM). This study was initiated with the goal of developing paleogeographic constraints from the package of sedimentary rocks that post-date the underlying volcanic rocks from which paleomagnetic poles have led to a late Mesoproterozoic apparent polar wander path for North America. Constraining the age of the remanence is critical to this effort.

A common approach to classify hematite grains within red beds is into a fine-grained pigmentary population, typically interpreted to have formed within the sediment, and a coarser-grained population that has been referred to in the literature as “specularite” (Butler, 1992; Van Der Voo & Torsvik, 2012). Tauxe et al. (1980) showed that sediments with abundant red pigmentary hematite in the Miocene Siwalik Group had lower thermal unblocking temperatures than gray samples dominated by coarser-grained specularite. An additional approach taken by Tauxe et al. (1980), and other workers going back to the work of Collinson (1965), is to preferentially remove

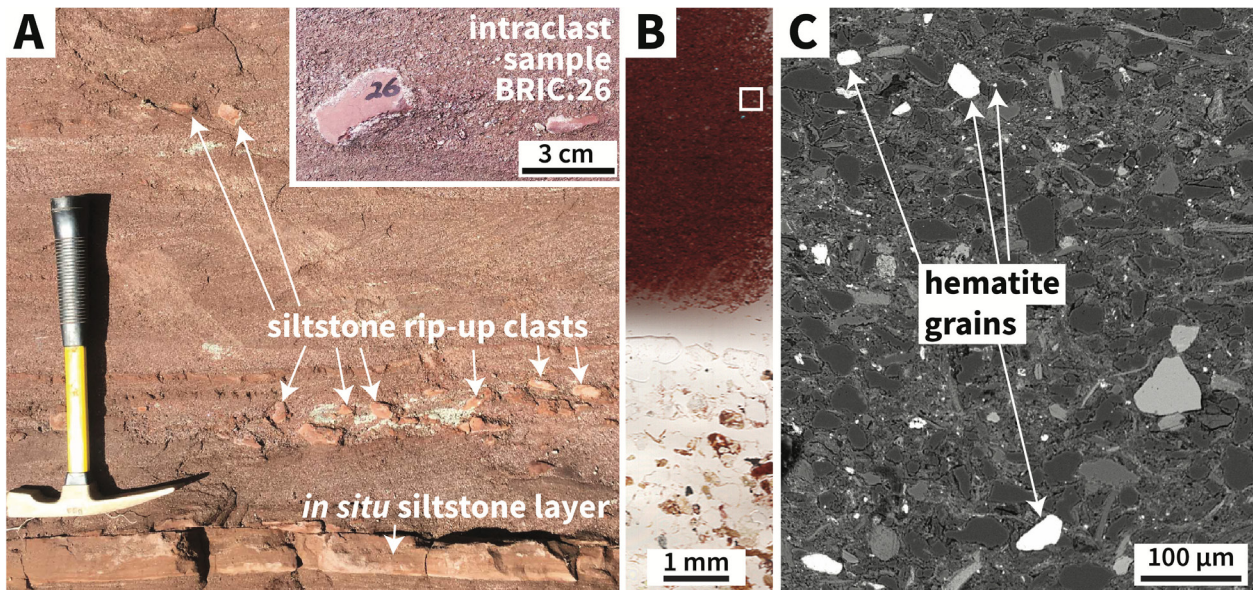


Fig. 1. (a) Siltstone intraclasts within the Freda Formation. The field photo shows an intact layer of siltstone below the hammer head, which is topped by a bed of trough cross-stratified coarse-grained sandstone with horizons of siltstone intraclasts. The hammer is 40 cm long. (b) A scan of a thin section of the BRIC.26 intraclast (upper half of image) and the coarse sand matrix (lower half of image). The red color of the intraclast is due to pigmentary hematite. (c) Backscatter electron image of the siltstone clast from the region of the white box in (b). The light-colored detrital grains that are labeled with arrows were confirmed to be hematite through electron backscatter diffraction.

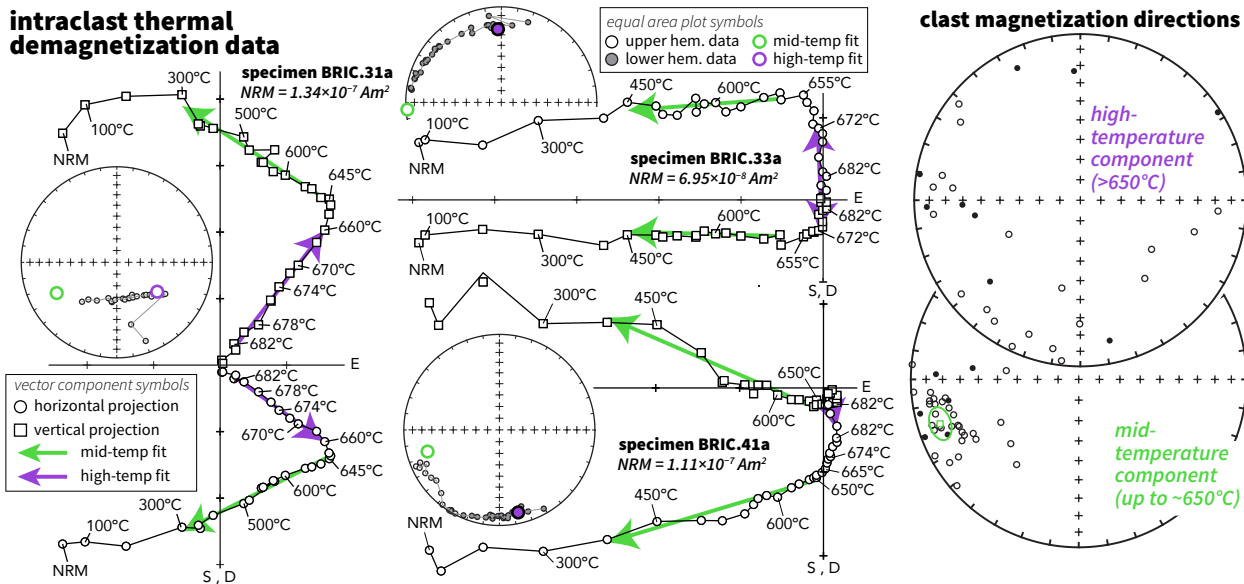
fine-grained pigmentary hematite through immersion in HCl acid. Paired chemical and thermal demagnetization data have been interpreted to show that pigmentary hematite removal coincides with removal of hematite with lower unblocking temperatures. These data support the interpretation that coarser grains more resistant to dissolution in acid correspond with those that carry remanence to the highest unblocking temperatures (Bilardello & Kodama, 2010; Tauxe et al., 1980) although simultaneous dissolution of fine and coarser hematite can occur (Jiang et al., 2017). Observations such as these have led to the practice of defining the characteristic remanent magnetization from hematite-bearing sediments as that held by the highest unblocking temperatures (Van Der Voo & Torsvik, 2012). Additional lines of evidence from field and lab based studies have supported this approach. For example, in the well-studied Carboniferous Mauch Chunk Formation of Pennsylvania, remanence removed up to ~660°C has uniform polarity and fails a fold test while the component removed upward of 670°C is dual polarity, was acquired before folding, and is interpreted as a primary magnetization (DiVenere & Opdyke, 1991; Kent & Opdyke, 1985). The work of Jiang et al. (2015) on the thermal demagnetization characteristics of hematite experimentally synthesized through ferrihydrite–hematite conversion provides additional support for discriminating between CRM and DRM on the basis of unblocking temperature. Nevertheless, the primary versus secondary nature of micron-scale specularite grains that carry the high-unblocking temperature remanence has been one of the largest sources of contention in the red bed controversy (Tauxe et al., 1980; Butler, 1992; Van Der Voo & Torsvik, 2012).

It can be difficult to reliably constrain the relative age of hematite within sedimentary rocks given that traditional paleomagnetic field tests can be ambiguous. A structural fold test can constrain whether remanence acquisition

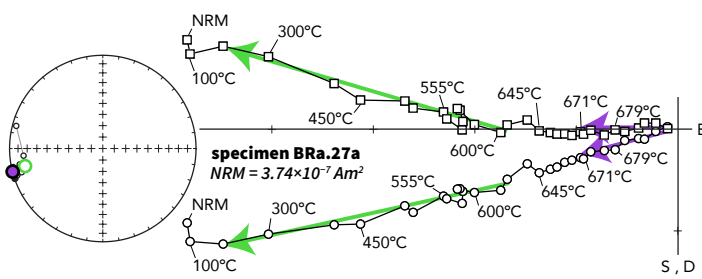
occurred prior to folding, but millions of years have typically passed between deposition and tilting. Dual-polarity directions through a sedimentary succession are often interpreted to indicate that the remanence records primary or near-primary magnetization. However, hematite growth could occur after deposition during a protracted period over which the geomagnetic field was in both reversed and normal polarities. What is needed to most confidently address the timing of remanence acquisition is a process that reorients the sediment before it has been fully lithified. One such process is when intraclasts composed of the lithology of interest have been liberated and redeposited within the depositional environment. Such intraclasts can provide significant insight into whether magnetization was acquired before or after reorientation as was done in Tauxe et al. (1980) and Opdyke and DiVenere (2004). While such clasts can be difficult to find and sample, we luckily found excellent exposures of siltstone intraclasts that were eroded from a coexisting lithofacies and redeposited within channel sandstone of the Freda Formation along the Bad River in northern Wisconsin (Fig. 1).

High-resolution thermal demagnetization on these clasts that we conducted in our paleomagnetism lab at Berkeley constrain the timing of hematite acquisition by revealing a component that formed prior to the erosion of the clasts within the depositional environment and another component that formed following their redeposition (Fig. 2). The primary component that unblocked in a narrow temperature range between 665 and 690°C has dispersed directions among the intraclasts indicating that the magnetization was rotated along with the clasts in the depositional environment. The secondary component unblocked over a broad temperature range from 100 up to 650°C or higher and has a consistent direction throughout the intraclasts indicating that it formed following deposition. During the visiting fellowship at the IRM, backfield demagnetization experiments were conducted on a Princeton Measurements

## intraclast thermal demagnetization data



## in-place siltstone thermal demagnetization data



## in-place siltstone directions

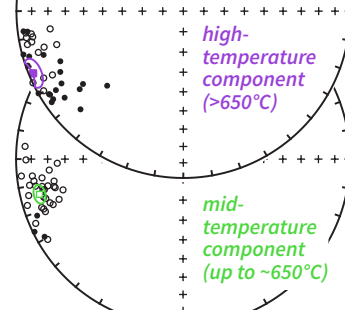


Fig. 2. Paleomagnetic data from intraclasts and in-place rocks of the same lithology reveal a mid-temperature component (green symbols) that typically unblocks prior to 655°C and a high-temperature component (purple symbols) that typically unblocks between 655 and 687°C. These components are present as varying fractions of the overall remanence. The high-temperature component directions from the clasts are dispersed indicating that the magnetization was acquired before the clasts were ripped up in the depositional environment. The mid-temperature component directions are clustered indicating that the magnetization was acquired in the clasts as a chemical remanence following deposition. The in-place siltstone show similar, but distinct directions between the two components consistent with the mid-temperature component being acquired following burial during an interval of rapid North American plate motion.

vibrating sample magnetometer and used to develop coercivity spectra. These spectra were modeled using the Max UnMix software package (Maxbauer et al., 2016; Figure 3). These spectra are well fit with two overlapping log-normal distributions associated with two populations of grains. One population has a median coercivity of ~300 mT and a distribution that extends from the lowest to the highest coercivities. The other population has a higher median coercivity of ~700 mT and a coercivity distribution that is limited to the high-coercivity range (purple curve in Figure 3). The high-coercivity phase can be considered to correspond with the plateau of high coercivities observed for single-domain hematite in the ~10 to ~100- $\mu\text{m}$  range (Özdemir & Dunlop, 2014; Fig. 4). The coercivity associated with the lower coercivity population (green curve in Figure 3) spans a large range which is consistent with a population of fine-grained authigenic hematite. Coercivity values for hematite become progressively larger from the superparamagnetic/stable-single-domain boundary up to grains sizes of ~300 nm (Özdemir & Dunlop, 2014; Fig. 4) overlapping with that associated with a coarser-grained detrital component.

Given the directional consistency of the mid-temperature component among the intraclasts (Fig. 2), this component

must have dominantly formed as a chemical remanent magnetization after the intraclasts were redeposited in the channel. Chemical remanent magnetization acquisition by pigmentary hematite would have occurred as hematite grains grew to sizes above the superparamagnetic to stable single-domain transition resulting in the wide range of unblocking temperatures that is observed. Low-temperature hysteresis experiments conducted at the IRM revealed an increase in remanent magnetization at low-temperature suggesting the presence of a population of superparamagnetic grains. The coercivity spectra are consistent with a population of hematite that has a wide coercivity range extending from low coercivities up to high coercivities (the green component in the unmixing models of Figure 3) which is likely associated with a population of authigenic hematite nanoparticles. In contrast, the sharp unblocking temperature close to the Néel temperature of the high-temperature component indicates that it is dominantly held by hematite grains that are >400 nm (based on Néel relaxation theory; Figure 4) such as the silt-sized hematite grains observed petrographically (Figure 1). The high-coercivity population within the coercivity spectra (purple curves in Figure 3) is consistent with this grain-size interpretation (Figure 4).

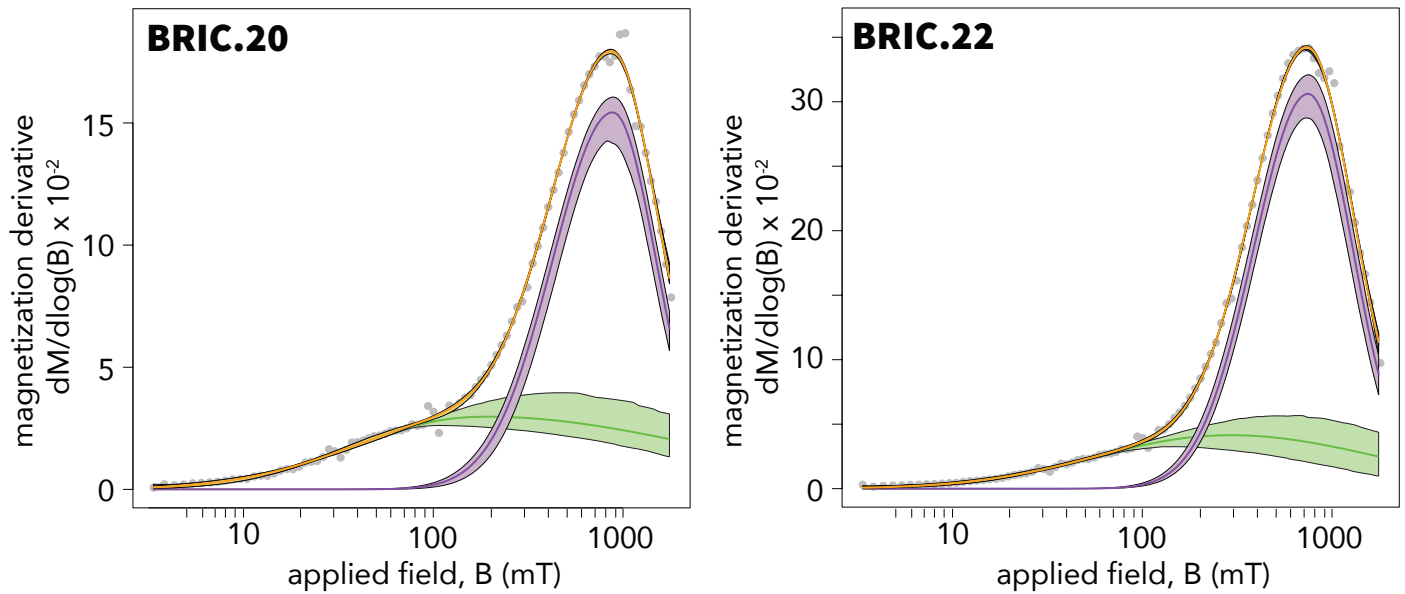


Fig. 3. Coercivity spectra developed from backfield demagnetization curves on BRIC intraclast specimens with the points being the data. The data were modeled using log-Gaussian distributions implemented with the Max UnMix software package (Maxbauer et al., 2016). The coercivity spectra can be well explained with two distributions: the higher coercivity distribution in purple and the lower coercivity distribution in green.

The differential unblocking temperature spectra of the two components within the Freda intraclasts provide strong support for the argument that chemical and detrital remanent magnetization can be distinguished due to detrital remanence unblocking at the highest temperatures. However, the Freda intraclast data also show that while the detrital remanent magnetization can be well isolated at temperatures as low as 650°C (specimen BRIC.31a in Figure 2), the chemical remanent magnetization thermal unblocking spectra can overlap with that of the detrital remanence and extend up to temperatures closer to the Néel temperature (specimen BRIC.41a in Figure 2). Therefore, to isolate primary remanence in red beds, best practice should be to proceed with very high resolution thermal demagnetization steps above 600°C, and particularly above 650°C. Characteristic remanence magnetization directions associated with hematite that are fit to compo-

nents that span a wide range of unblocking temperatures including those lower than ~650°C are likely convolving a pigmentary chemical remanence and a detrital remanence held by larger grains.

Overall, the data support the interpretation that magnetizations of hematite-bearing sedimentary rocks held by >400-nm grains that unblock close to the Néel temperature are more likely to record magnetization from the time of deposition. Hydrodynamic sorting associated with the delivery of detrital hematite will lead to a narrower and coarser size distribution of grains than that of authigenic pigmentary hematite growth. This primary magnetization can be successfully isolated from co-occurring authigenic hematite through thermal demagnetization provided such thermal demagnetization is performed at high-resolution.

The results from this study were published in: Swanson-

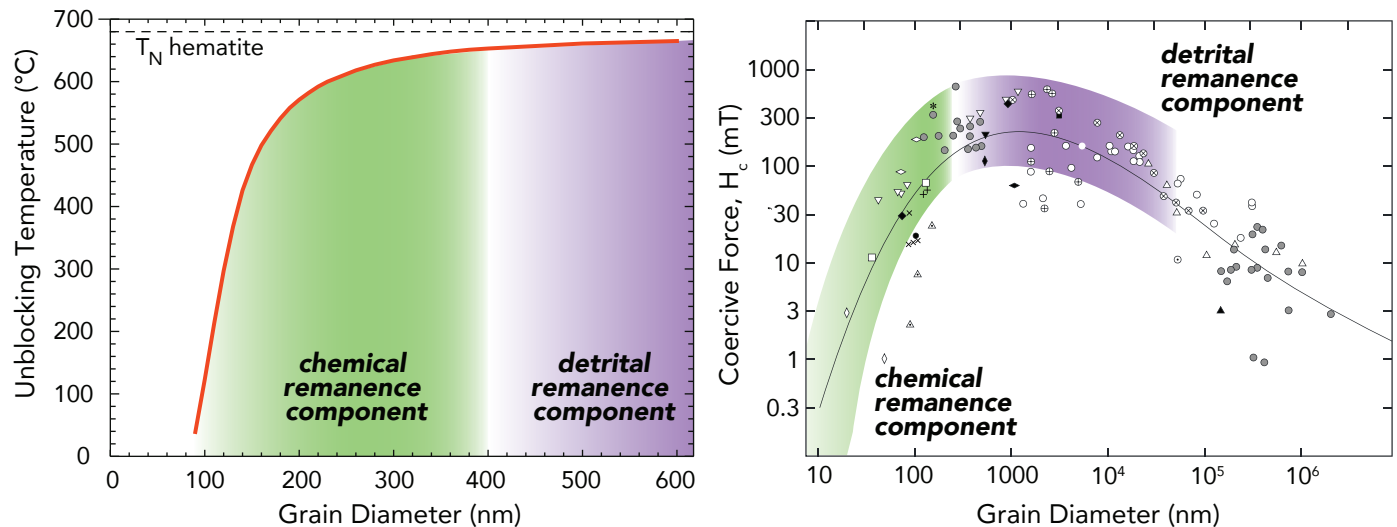


Fig. 4. (left) Calculated unblocking temperatures using Néel thermal relaxation theory of idealized spherical hematite grains using a thermal fluctuation rate of  $10^{10} \text{ s}^{-1}$  and a relaxation time of 5 min for comparison to thermal demagnetization data (modified from Swanson-Hysell et al., 2011). The unblocking temperatures of the mid-temperature chemical component (green) and the high-temperature detrital component (purple) are shown and can be used to infer grain size. Compilation of coercivity data from hematite as a function of grain diameter from Özdemir and Dunlop (2014). The higher coercivity population from Figure 3 corresponds to the larger grain sizes than the lower coercivity component associated with the chemical remanence.

Hysell, N. L., Fairchild, L. M., & Slotznick, S. P. (2019). Primary and secondary red bed magnetization constrained by fluvial intraclasts. *Journal of Geophysical Research: Solid Earth*, 124. <https://doi.org/10.1029/2018JB017067>. Portions of the text in this report are taken and adapted from that paper. The reader is encouraged to seek it out for additional details. An open access version of the manuscript is available here: <https://escholarship.org/uc/item/619097rn>

## References

- Bilardello, D., & Kodama, K. P. (2010a). Palaeomagnetism and magnetic anisotropy of Carboniferous red beds from the Maritime Provinces of Canada: Evidence for shallow palaeomagnetic inclinations and implications for North American apparent polar wander. *Geophysical Journal International*, 180(3), 1013–1029. <https://doi.org/10.1111/j.1365-246x.2009.04457.x>
- Butler, R. (1992). *Paleomagnetism: Magnetic domains to geologic terranes*. Boston: Blackwell Scientific Publications.
- Collinson, D. W. (1965). Origin of remanent magnetization and initial susceptibility of certain red sandstones. *Geophysical Journal International*, 9(2-3), 203–217. <https://doi.org/10.1111/j.1365-246x.1965.tb02071.x>
- DiVenere, V. J., & Opdyke, N.D. (1991). Magnetic polarity stratigraphy in the uppermost Mississippian Mauch Chunk Formation, Pottsville, Pennsylvania. *Geology*, 19(2), 127. [https://doi.org/10.1130/0091-7613\(1991\)019<0127:mpsitu>2.3.co;2](https://doi.org/10.1130/0091-7613(1991)019<0127:mpsitu>2.3.co;2)
- Jiang, Z., Liu, Q., Dekkers, M. J., Tauxe, L., Qin, H., Barrón, V., & Torrent, J. (2015). Acquisition of chemical remanent magnetization during experimental ferrihydrite–hematite conversion in Earth-like magnetic field—Implications for paleomagnetic studies of red beds. *Earth and Planetary Science Letters*, 428, 1–10. <https://doi.org/10.1016/j.epsl.2015.07.024>
- Kent, D. V., & Opdyke, N. D. (1985). Multicomponent magnetizations from the Mississippian Mauch Chunk Formation of the central Appalachians and their tectonic implications. *Journal of Geophysical Research*, 90(B7), 5371–5383. <https://doi.org/10.1029/jb090ib07p05371>
- Maxbauer, D. P., Feinberg, J. M., & Fox, D. L. (2016). MAX UnMix: A web application for unmixing magnetic coercivity distributions. *Computers and Geosciences*, 95, 140–145. <https://doi.org/10.1016/j.cageo.2016.07.009>
- Opdyke, N. D., & DiVenere, V. J. (2004). The magnetic polarity stratigraphy of the Mauch Chunk Formation, Pennsylvania. *Proceedings of the National Academy of Sciences*, 101(37), 13,423–13,427. <https://doi.org/10.1073/pnas.0403786101>
- Özdemir, Ö., & Dunlop, D. J. (2014). Hysteresis and coercivity of hematite. *Journal of Geophysical Research: Solid Earth*, 119, 2582–2594. <https://doi.org/10.1002/2013JB010739>
- Swanson-Hysell, N. L., Feinberg, J. M., Berquó, T. S., & Maloof, A. C. (2011). Self-reversed magnetization held by martite in basalt flows from the 1.1-billion-year-old Keweenaw rift, Canada. *Earth and Planetary Science Letters*, 305(1-2), 171–184. <https://doi.org/10.1016/j.epsl.2011.02.053>
- Tauxe, L., Kent, D. V., & Opdyke, N. D. (1980). Magnetic components contributing to the NRM of middle siwalik red beds. *Earth and Planetary Science Letters*, 47, 279–284. [https://doi.org/10.1016/0012-821X\(80\)90044-8](https://doi.org/10.1016/0012-821X(80)90044-8)
- Van Der Voo, R., & Torsvik, T. H. (2012). The history of remagnetization of sedimentary rocks: Deceptions, developments and discoveries. *Geological Society, London, Special Publications*, 371(1), 23–53. <https://doi.org/10.1144/SP371.2>

# Visiting Fellows

January - June, 2020

## Annemarieke Beguin

Utrecht University

*Do dendritic iron-oxide grains behave as series of noninteracting single domain grains in paleointensity experiments?*

## Natalia Bezaeva

Kazan Federal University

*Magnetic characterization of impactites from Karla impact structure and impact glasses from Popigai impact structure, Russia*

## Liao Chang

Peking University

*Investigating magnetic fabrics within the Beaver Bay Complex, Northeastern Minnesota and their relationships to the 1.1 Ga Midcontinent Rift*

## Evan Hamilton

University of Oklahoma

*Occurrence and Origin of Strongly Negative Field-Dependence of AC Magnetic Susceptibility*

## Louise Koornneef

University of Plymouth

*Hydrothermal influences on magnetic mineral assemblages in marine sediments (Guaymas Basin, Gulf of California, IODP Expedition 385)*

## Grant Rea-Downing

University of Utah

*Testing magnetic techniques to estimate the particle size distribution and composition of Fe-bearing particulate matter in air pollution from the Salt Lake Valley, Utah.*

## Shishun Wang

Peking University

*Quantifying hydrothermal alteration on basaltic ocean crust through multiple rock magnetic properties*

## Yiming Zhang\*

UC Berkeley

*Paleomagnetism and rock magnetism study on Mesoproterozoic Beaver Bay Complex and anorthosite xenoliths therein*

\*U.S. Student Fellows

# Current Articles

A list of current research articles dealing with various topics in the physics and chemistry of magnetism is a regular feature of the IRM Quarterly. Articles published in familiar geology and geophysics journals are included; special emphasis is given to current articles from physics, chemistry, and materials-science journals. Most are taken from INSPEC (© Institution of Electrical Engineers), Geophysical Abstracts in Press (© American Geophysical Union), and The Earth and Planetary Express (© Elsevier Science Publishers, B.V.), after which they are subjected to Procrustean culling for this newsletter. An extensive reference list of articles (primarily about rock magnetism, the physics and chemistry of magnetism, and some paleomagnetism) is continually updated at the IRM. This list, with more than 10,000 references, is available free of charge. Your contributions both to the list and to the Current Articles section of the IRM Quarterly are always welcome.

## Anisotropy and Magnetic Fabrics

- Biedermann, A. R. Magnetic Pore Fabrics: The Role of Shape and Distribution Anisotropy in Defining the Magnetic Anisotropy of Ferrofluid-Impregnated Samples, *Geochemistry Geophysics Geosystems*.
- Heij, G. W., and R. D. Elmore (2019), The magnetic fabric of the Wolfcamp shale, Midland Basin, west Texas: Understanding petrofabric variability, hydrocarbon associations, and iron enrichment, *Aapg Bulletin*, 103(11), 2785-2806.
- Issachar, R., R. Weinberger, G. I. Alsop, and T. Levi Deformation of Intrasalt Beds Recorded by Magnetic Fabrics, *Journal of Geophysical Research-Solid Earth*.
- Li, W. J., H. J. Xu, and J. F. Zhang Magnetic Fabric and Petrofabric of Amphibolites from the Namcha Barwa Complex, Eastern Himalaya, *Journal of Earth Science*.
- Tomek, F., A. K. Gilmer, M. S. Petronis, P. W. Lipman, and M. S. Foucher (2019), Protracted Multipulse Emplacement of a Postresurgent Pluton: The Case of Platoro Caldera Complex (Southern Rocky Mountain Volcanic Field, Colorado), *Geochemistry Geophysics Geosystems*.
- Usui, Y., T. Yamazaki, T. Oka, and Y. Kumagai Inverse Magnetic Susceptibility Fabrics in Pelagic Sediment: Implications for Magnetofossil Abundance and Alignment, *Journal of Geophysical Research-Solid Earth*.
- Yang, T., X. X. Zhao, K. Petronotis, M. J. Dekkers, and H. R. Xu Anisotropy of Magnetic Susceptibility (AMS) of Sediments From Holes U1480E and U1480H, IODP Expedition 362: Sedimentary or Artificial Origin and Implications for Paleomagnetic Studies, *Geochemistry Geophysics Geosystems*.
- Zak, J., K. Verner, J. Jezek, and J. Trubac (2019), Complex mid-crustal flow within a growing granite-migmatite dome: An example from the Variscan belt illustrated by the anisotropy of magnetic susceptibility and fabric modelling, *Geological Journal*, 54(6), 3681-3699.

## Archeomagnetism

- Basavaiah, N. (2019), Rock Magnetic Research at IIG and its Application to Paleomagnetic, Archaeomagnetic and Environmental Magnetic Aspects, *Journal of the Geological Society of India*, 94(5), 550-550.
- Stele, A., J. W. E. Fassbinder, J. W. Hartling, J. Bussmann, J. Schmidt, and C. Zielhofer Genesis of magnetic anomalies and magnetic properties of archaeological sediments in floodplain wetlands of the Fossa Carolina, *Archaeological Prospection*.

## Chronostratigraphy/Magnetostratigraphy

- Dickinson, W. R. (2018), Tectonosedimentary Relations of Pennsylvanian to Jurassic Strata on the Colorado Plateau, in *Tectonosedimentary Relations of Pennsylvanian to Jurassic Strata on the Colorado Plateau*, edited, pp. 1-184.

- Gallet, Y., V. Pavlov, and I. Korovnikov (2019), Extreme geomagnetic reversal frequency during the Middle Cambrian as revealed by the magnetostratigraphy of the Khorbusuonka section (northeastern Siberia), *Earth and Planetary Science Letters*, 528.
- Gao, P., J. S. Nie, M. S. Li, and P. Li Confirmation of a Late Miocene Subchron C4n.2n-1r From the Eastern Qaidam Basin in the NE Tibetan Plateau, *Journal of Geophysical Research-Solid Earth*.
- Gastaldo, R. A., J. Neveling, J. W. Geissman, and C. V. Looy (2019), Testing the daptoccephalus and lystrosaurus assemblage zones in a lithostratigraphic, magnetostratigraphic, and palynological framework in the free state, South Africa, *Palaos*, 34(11), 542-561.
- Hoshi, H., H. Iwano, T. Danhara, H. Oshida, H. Hayashi, Y. Kurihara, and Y. Yanagisawa (2019), Age of the N7/N8 (M4/M5) planktonic foraminifera zone boundary: constraints from the zircon geochronology and magnetostratigraphy of early Miocene sediments in Ichishi, Japan, *Chemical Geology*, 530.
- Ivanova, E., D. Borisov, O. Dmitrenko, and I. Murdmaa (2020), Hiatuses in the late Pliocene-Pleistocene stratigraphy of the Ioffe calcareous contourite drift, western South Atlantic, *Marine and Petroleum Geology*, 111, 624-637.
- Kent, D. V., P. E. Olsen, C. Lepre, C. Rasmussen, R. Mundil, G. E. Gehrels, D. Giesler, R. B. Irmis, J. W. Geissman, and W. G. Parker Magnetostratigraphy of the Entire Chinle Formation (Norian Age) in a Scientific Drill Core From Petrified Forest National Park (Arizona, USA) and Implications for Regional and Global Correlations in the Late Triassic, *Geochemistry Geophysics Geosystems*.
- Kodama, K. P. (2019), Rock Magnetic Cyclostratigraphy of the Carboniferous Mauch Chunk Formation, Pottsville, PA, United States, *Frontiers in Earth Science*, 7.
- Lapointe, F., P. Francus, J. S. Stoner, M. B. Abbott, N. L. Balascio, T. L. Cook, R. S. Bradley, S. L. Forman, M. Besonen, and G. St-Onge (2019), Chronology and sedimentology of a new 2.9 ka annually laminated record from South Sawtooth Lake, Ellesmere Island, *Quaternary Science Reviews*, 222.
- Nie, J. S., X. P. Ren, J. E. Saylor, Q. D. Su, B. K. Horton, M. A. Bush, W. H. Chen, and K. Pfaff (2020), Magnetic polarity stratigraphy, provenance, and paleoclimate analysis of Cenozoic strata in the Qaidam Basin, NE Tibetan Plateau, *Geological Society of America Bulletin*, 132(1-2), 310-320.
- Yan, J. Y., J. M. Hu, W. B. Gong, X. B. Liu, Y. G. Yin, and C. Tan Late Cenozoic magnetostratigraphy of the Yuncheng Basin, central North China Craton and its tectonic implications, *Geological Journal*.
- Yang, F., Z. T. Guo, C. X. Zhang, S. A. Md, Z. L. He, and C. L. Deng (2019), High-Resolution Eocene Magnetostratigraphy of the Xijigou Section: Implications for the Infilling Process of Xining Basin, Northeastern Tibetan Plateau, *Journal of Geophysical Research-Solid Earth*, 124(8), 7588-7603.
- Zhang, W. L., et al. (2020), Magnetostratigraphic constraints on the age of the Hippurion fauna in the Linxia Basin of China, and its implications for stepwise aridification, *Palaeogeography Palaeoclimatology Palaeoecology*, 537.

## Environmental Magnetism and Paleoclimate Proxies

- Abubakar, R., A. R. Muxworthy, A. Fraser, M. A. Sephton, J. S. Watson, D. Heslop, G. A. Paterson, and P. Southern (2020), Mapping hydrocarbon charge-points in the Wessex Basin using seismic, geochemistry and mineral magnetics, *Marine and Petroleum Geology*, 111, 510-528.
- Badesab, F., V. Gaikwad, and P. Dewangan (2019), Controls on greigit preservation in a gas hydrate system of the Krishna-Godavari basin, Bay of Bengal, *Geo-Marine Letters*.
- Ben Ameer, M., S. Masmoudi, A. Abichou, M. Medhioub, and C. Yaich (2019), Use of the magnetic, geochemical, and sedimentary records in establishing paleoclimate change in the environment of Sebkhah: Case of the Sebkhah Mhabeul in southeastern Tunisia, *Comptes Rendus Geoscience*, 351(7), 487-497.
- Benaiges-Fernandez, R., J. Palau, F. G. Offeddu, J. Cama, J. Urmeneta, J. M. Soler, and B. Dold (2019), Dissimilatory bioreduction of iron(III) oxides by *Shewanella loihica* under marine sediment conditions, *Marine Environmental Research*, 151.
- Bradak, B., Y. Seto, and J. Nawrocki (2019), Significant pedogenic and palaeoenvironmental changes during the early Middle Pleistocene in Central Europe, *Palaeogeography Palaeoclimatology Palaeoecol-*

- ogy, 534.
- Capraro, L., F. Tateo, P. Ferretti, E. Fornaciari, P. Macri, D. Scarponi, N. Preto, F. Xian, X. H. Kong, and X. J. Xie (2019), A Mediterranean perspective on Be-10, sedimentation and climate around the Matuyama/Brunhes boundary: les liaisons dangereuses?, *Quaternary Science Reviews*, 226.
- Chanda, P., Z. Zhou, D. E. Latta, M. M. Scherer, B. L. Beard, and C. M. Johnson (2020), Effect of organic C on stable Fe isotope fractionation and isotope exchange kinetics between aqueous Fe(II) and ferrihydrite at neutral pH, *Chemical Geology*, 531.
- Clague, J. J., R. W. Barendregt, B. Menounos, N. J. Roberts, J. Rabassa, O. Martinez, B. Ercolano, H. Corbella, and S. R. Hemming (2020), Pliocene and Early Pleistocene glaciation and landscape evolution on the Patagonian Steppe, Santa Cruz province, Argentina, *Quaternary Science Reviews*, 227.
- Gautam, P., P. Huyghe, J. L. Mugnier, and K. R. Regmi Magnetochemical signature of the Lower-to-Middle Siwaliks transition in the Karnali River section (Western Nepal): Implications for Himalayan tectonics and climate, *Geological Journal*.
- Giaccio, B., et al. (2019), Extending the tephra and palaeoenvironmental record of the Central Mediterranean back to 430 ka: A new core from Fucino Basin, central Italy, *Quaternary Science Reviews*, 225.
- Haiblen, A. M., B. N. Opdyke, A. P. Roberts, D. Heslop, and P. A. Wilson (2019), Midlatitude Southern Hemisphere Temperature Change at the End of the Eocene Greenhouse Shortly Before Dawn of the Oligocene Icehouse, *Paleoceanography and Paleoclimatology*.
- Hajna, N. Z., B. Otonicar, P. Pruner, M. Culiberg, J. Hlavac, O. Mandic, R. Skala, and P. Bosak (2019), Late Pleistocene lacustrine sediments and their relation to red soils in the northeastern margin of the Dinaric karst, *Acta Carsologica*, 48(2), 153-171.
- Hu, C. S., W. H. Li, L. Cao, G. L. Xu, and Y. Q. Zhou (2019), Evidence for wetter climate recorded in the Jingxian red clay section since approximately 840 ka ago and its relationship with the East Asian summer monsoon intensity, *Quaternary International*, 532, 57-65.
- Hu, X. F., J. L. Zhao, P. F. Zhang, Y. Xue, B. N. An, F. Huang, H. M. Yu, G. L. Zhang, and X. J. Liu (2019), Fe isotopic composition of the Quaternary Red Clay in subtropical Southeast China: Redoxic Fe mobility and its palaeoenvironmental implications, *Chemical Geology*, 524, 356-367.
- Huang, W. T., M. J. Jackson, M. J. Dekkers, P. Solheid, B. Zhang, Z. J. Guo, and L. Ding (2019), Nanogoethite as a Potential Indicator of Remagnetization in Red Beds, *Geophysical Research Letters*, doi:10.1029/2019GL084715.
- Huang, Y. S., et al. (2019), Hydrothermal activity revealed by rock magnetic anomaly from core sediments in the southern Okinawa Trough, *Terrestrial Atmospheric and Oceanic Sciences*, 30(5), 685-694.
- Le Nagard, L., et al. (2019), Magnetite magnetosome biomineralization in *Magnetospirillum magneticum* strain AMB-1: A time course study, *Chemical Geology*, 530.
- Lepre, C. J. Constraints on Fe-Oxide Formation in Monsoonal Vertisols of Pliocene Kenya Using Rock Magnetism and Spectroscopy, *Geochemistry Geophysics Geosystems*.
- Li, M. X., H. B. Liu, T. H. Chen, L. Wei, C. Wang, W. Hu, and H. L. Wang (2019), The transformation of alpha-(Al, Fe)OOH in natural fire: Effect of Al substitution amount on fixation of phosphate, *Chemical Geology*, 524, 368-382.
- Li, Q., Q. Zhang, G. X. Li, Q. S. Liu, M. T. Chen, J. S. Xu, and J. H. Li (2019), A new perspective for the sediment provenance evolution of the middle Okinawa Trough since the last deglaciation based on integrated methods, *Earth and Planetary Science Letters*, 528.
- Li, M. T., H. J. Song, P. B. Wignall, Z. B. She, X. Dai, H. Y. Song, and Q. Xiao (2019), Early Triassic oceanic red beds coupled with deep sea oxidation in South Tethys, *Sedimentary Geology*, 391.
- Liu, Y. H., X. S. Wang, Y. H. Guo, Y. M. Mao, and H. Li (2019), Association of black carbon with heavy metals and magnetic properties in soils adjacent to a cement plant, Xuzhou (China), *Journal of Applied Geophysics*, 170.
- Liu, M., D. Z. Chen, X. Q. Zhou, D. J. Tang, T. R. Them, and M. S. Jiang (2019), Upper Ordovician marine red limestones, Tarim Basin, NW China: A product of an oxygenated deep ocean and changing climate?, *Global and Planetary Change*, 183.
- Maxbauer, D. P., M. D. Shapley, C. E. Geiss, and E. Ito Holocene climate recorded by magnetic properties of lake sediments in the Northern Rocky Mountains, USA, Holocene.
- Mitra, K., and J. G. Catalano Chlorate as a Potential Oxidant on Mars: Rates and Products of Dissolved Fe(II) Oxidation, *Journal of Geophysical Research-Planets*.
- Notini, L., D. E. Latta, A. Neumann, C. I. Pearce, M. Sassi, A. T. N'Diaye, K. M. Rosso, and M. M. Scherer (2019), A Closer Look at Fe(II) Passivation of Goethite, *Acs Earth and Space Chemistry*, 3(22), 2717-2725.
- Ojala, A. E. K., J. Mattila, J. Hamalainen, and R. Sutinen (2019), Lake sediment evidence of paleoseismicity: Timing and spatial occurrence of late- and postglacial earthquakes in Finland, *Tectonophysics*, 771.
- Pas, D., A. C. Da Silva, G. Poulain, S. Spassov, and F. Boulvain (2019), Magnetic Susceptibility Record in Paleozoic Succession (Rhenocynian Massif, Northern Europe) - Disentangling Sea Level, Local and Diagenetic Impact on the Magnetic Records, *Frontiers in Earth Science*, 7.
- Sabbeth, L., B. P. Wernicke, T. D. Raub, J. A. Grover, E. B. Lander, and J. L. Kirschvink (2019), Grand Canyon provenance for orthoquartzite clasts in the lower Miocene of coastal southern California, *Geosphere*, 15(6), 1973-1998.
- Seiriene, V., P. Sinkunas, M. Stancikaite, D. Kisieliene, and L. Gedminiene (2019), Late Middle Pleistocene interglacial sediments from Buivydziai site, eastern Lithuania: A problem of chronostratigraphic correlation, *Quaternary International*, 534, 18-29.
- Sharma, C. P., S. L. Rawat, P. Srivastava, N. K. Meena, R. Agnihotri, A. Kumar, P. Chahal, S. K. S. Gahlaud, and U. K. Shukla High-resolution climatic (monsoonal) variability reconstructed from a continuous similar to 2700-year sediment record from Northwest Himalaya (Ladakh), Holocene.
- Shchetnikov, A. A., et al. (2019), Upper Paleolithic site Tuyana - a multiproxy record of sedimentation and environmental history during the Late Pleistocene and Holocene in the Tunka rift valley, Baikal region, *Quaternary International*, 534, 138-157.
- Silva, L. S., J. Marques, V. Barron, R. P. Gomes, D. D. Teixeira, D. S. Siqueira, and V. Vasconcelos (2020), Spatial variability of iron oxides in soils from Brazilian sandstone and basalt, *Catena*, 185.
- Smith, K. F., et al. (2019), Plutonium(IV) Sorption during Ferrihydrite Nanoparticle Formation, *Acs Earth and Space Chemistry*, 3(11), 2437-2442.
- van der Boon, A., R. van der Ploeg, M. J. Cranwinckel, K. F. Kuiper, S. V. Popov, I. P. Tabachnikova, D. V. Palcu, and W. Krijgsman (2019), Integrated stratigraphy of the Eocene-Oligocene deposits of the northern Caucasus (Belaya River, Russia): Intermittent oxygen-depleted episodes in the Peri-Tethys and Paratethys, *Palaeogeography Palaeoclimatology Palaeoecology*, 536.
- Vodyanitskii, Y. N., and T. M. Minkina (2019), Non-stable Fe minerals in waterlogged soils, *Applied Geochemistry*, 110.
- Voelz, J. L., N. W. Johnson, C. L. Chun, W. A. Arnold, and R. L. Penn (2019), Quantitative Dissolution of Environmentally Accessible Iron Residing in Iron-Rich Minerals: A Review, *Acs Earth and Space Chemistry*, 3(8), 1371-1392.
- Wang, L. S., S. Y. Hu, G. Yu, X. H. Wang, M. M. Ma, M. N. Liao, Q. Wang, and Z. H. Zhang (2019), Evolution of the radial sand ridge field in the southwestern Yellow Sea, China since the late MIS 3, *Zeitschrift Fur Geomorphologie*, 62(3), 217-229.
- Wogau, K. H., H. W. Arz, H. N. Bohnel, N. R. Nowaczyk, and J. Park (2019), High resolution paleoclimate and paleoenvironmental reconstruction in the Northern Mesoamerican Frontier for Prehistory to Historical times, *Quaternary Science Reviews*, 226.
- Zhang, T. W., X. Q. Yang, Q. Chen, J. L. Toney, Q. X. Zhou, and H. H. Gao Humidity variations spanning the 'Little Ice Age' from an upland lake in southwestern China, Holocene.
- Zhang, Q., Q. S. Liu, A. P. Roberts, J. C. Larrasoana, X. F. Shi, and C. S. Jin (2020), Mechanism for enhanced eolian dust flux recorded in North Pacific Ocean sediments since 4.0 Ma: Aridity or humidity at dust source areas in the Asian interior?, *Geology*, 48(1), 77-81.
- Zhang, L. M., Q. Zeng, X. Liu, P. Chen, X. X. Guo, L. Y. Z. Ma, H. L. Dong, and Y. Huang (2019), Iron reduction by diverse actinobacteria under oxic and pH-neutral conditions and the formation of secondary minerals, *Chemical Geology*, 525, 390-399.
- Zhang, Y., A. R. Muxworthy, D. Jia, G. Q. Wei, B. Xia, B. Wen, M. M. Wang, W. L. Liu, and M. J. Brzozowski (2019), Identifying and Dating the Destruction of Hydrocarbon Reservoirs Using Secondary Chemical Remanent Magnetization, *Geophysical Research Letters*, 46(20), 11100-11108.
- Zheng, X. F., B. Luu, Z. X. Chen, X. Y. Ma, and G. Y. Zhao (2019), A comparative analysis of magnetic properties of subtropical red

soil derived from different weathering crusts, *Chinese Journal of Geophysics-Chinese Edition*, 62(9), 3509-3523.

Zhuang, L., Z. Y. Tang, Z. Yu, J. Li, and J. Tang (2019), Methanogenic Activity and Microbial Community Structure in Response to Different Mineralization Pathways of Ferrihydrite in Paddy Soil, *Frontiers in Earth Science*, 7.

## Extraterrestrial Magnetism

Alfing, J., M. Patzek, and A. Bischoff (2019), Modal abundances of coarse-grained (> 5  $\mu\text{m}$ ) components within CI-chondrites and their individual clasts - Mixing of various lithologies on the CI parent body(ies), *Geochemistry*, 79(4).

Bates, H. C., A. J. King, K. L. D. Hanna, N. E. Bowles, and S. S. Russell Linking mineralogy and spectroscopy of highly aqueously altered CM and CI carbonaceous chondrites in preparation for primitive asteroid sample return, *Meteoritics & Planetary Science*.

Bischoff, A., et al. (2019), The Renchen L5-6 chondrite breccia - The first confirmed meteorite fall from Baden-Württemberg (Germany), *Geochemistry*, 79(4).

Li, S. J., S. J. Wang, B. K. Miao, Y. Li, X. Y. Li, X. J. Zeng, and Z. P. Xia The Density, Porosity, and Pore Morphology of Fall and Find Ordinary Chondrites, *Journal of Geophysical Research-Planets*.

Nava, J., M. D. Suttle, R. Spiess, L. Folco, J. Najorka, C. Carli, and M. Massironi Hydrothermal activity on the CV parent body: New perspectives from the giant Transantarctic Mountains minimetorite TAM5.29, *Meteoritics & Planetary Science*.

Rubin, A. E., and Y. Li (2019), Formation and destruction of magnetite in CO3 chondrites and other chondrite groups, *Geochemistry*, 79(4).

## Fundamental Rock Magnetism

Chang, L., R. J. Harrison, and T. A. Berndt (2019), Micromagnetic simulation of magnetofossils with realistic size and shape distributions: Linking magnetic proxies with nanoscale observations and implications for magnetofossil identification, *Earth and Planetary Science Letters*, 527.

Harrison, R. J., X. Zhao, P. X. Hu, T. Sato, D. Heslop, A. R. Muxworthy, H. Oda, V. S. C. Kuppili, and A. P. Roberts (2019), Simulation of Remanent, Transient, and Induced FORC Diagrams for Interacting Particles With Uniaxial, Cubic, and Hexagonal Anisotropy, *Journal of Geophysical Research-Solid Earth*.

Khakhalova, E., and B. M. Moskowitz (2019), High-Temperature Observation of Transdomain Transitions in Vortex States in Intermediate Titanomagnetite, *Journal of Geophysical Research-Solid Earth*, 124(8), 7604-7615.

Koulialias, D., B. Lesniak, M. Schwotzer, P. G. Weidler, J. F. Loffler, and A. U. Gehring The Besnus Transition in Single-Domain 4C Pyrrhotite, *Geochemistry Geophysics Geosystems*.

## Geomagnetism, Paleointensity and Records of the Magnetic Field

Ahn, H. S., and Y. Yamamoto (2019), Paleomagnetic study of basaltic rocks from Baengnyeong Island, Korea: efficiency of the Tsunakawa-Shaw paleointensity determination on non-SD-bearing materials and implication for the early Pliocene geomagnetic field intensity, *Earth Planets and Space*, 71(1).

Behnam, S., and H. Ramazi (2019), Interpretation of geomagnetic data using power spectrum and 3D modeling of Gol-e-Gohar magnetic anomaly, *Journal of Applied Geophysics*, 171.

Buffett, B., W. Davis, and M. S. Avery Variability of Millennial-Scale Trends in the Geomagnetic Axial Dipole, *Geophysical Research Letters*.

Fagre, M., B. S. Zossi, E. Yigit, H. Amit, and A. G. Elias High frequency sky wave propagation during geomagnetic field reversals, *Studia Geophysica Et Geodaetica*.

Herve, G., M. Perrin, L. M. Alva-Valdivia, A. Rodriguez-Trejo, A. Hernandez-Cardona, M. C. Tello, and C. M. Rodriguez Secular Variation of the Intensity of the Geomagnetic Field in Mexico During the First Millennium BCE, *Geochemistry Geophysics Geosystems*.

Kulakov, E. V., C. J. Sprain, P. V. Doubrovine, A. V. Smirnov, G. A. Paterson, L. Hawkins, L. Fairchild, E. J. Piispa, and A. J. Biggin (2019), Analysis of an Updated Paleointensity Database (Q(PI)-PINT) for 65-200 Ma: Implications for the Long-Term History of

Dipole Moment Through the Mesozoic, *Journal of Geophysical Research-Solid Earth*, 124(10), 9999-10022.

Li, G. H., D. S. Xia, E. Appel, H. Lu, Y. J. Wang, J. Jia, and X. Q. Yang (2020), Characteristics of a relative paleointensity record from loess deposits in arid central Asia and chronological implications, *Quaternary Geochronology*, 55.

Mahgoub, A. N., E. Juarez-Arriaga, H. Bohnel, L. R. Manzanilla, and A. Cyphers (2019), Refined 3600 years palaeointensity curve for Mexico, *Physics of the Earth and Planetary Interiors*, 296.

Panovska, S., M. Korte, and C. G. Constable One Hundred Thousand Years of Geomagnetic Field Evolution, *Reviews of Geophysics*.

Shcherbakov, V. P., S. K. Gribov, F. Lhuillier, N. A. Aphinogenova, and V. A. Tsel'movich (2019), On the Reliability of Absolute Paleointensity Determinations on Vasaltic Rocks Bearing a Thermochemical Remanence, *Journal of Geophysical Research-Solid Earth*, 124(8), 7616-7632.

## High Pressure Magnetism

Agarwal, A., and L. M. Alva-Valdivia (2019), Curie temperature of weakly shocked target basalts at the Lonar impact crater, India, *Earth Planets and Space*, 71(1).

Agarwal, A., A. Kontny, T. Kenkmann, and M. H. Poelchau (2019), Variation in Magnetic Fabrics at Low Shock Pressure Due to Experimental Impact Cratering, *Journal of Geophysical Research-Solid Earth*, 124(8), 9095-9108.

Henrichs, L. F., A. Kontny, B. Reznik, U. Gerhards, J. Gottlicher, T. Genssle, and F. Schilling Shock-induced formation of wustite and fayalite in a magnetite-quartz target rock, *Meteoritics & Planetary Science*.

## Instrumentation and Techniques

Berndt, T. A., and L. Chang Waiting for Forcot: Accelerating FORC Processing 100x Using a Fast-Fourier-Transform Algorithm, *Geochemistry Geophysics Geosystems*.

Heslop, D., and A. P. Roberts Quantifying the Similarity of Paleomagnetic Poles, *Journal of Geophysical Research-Solid Earth*.

Lurcock, P. C., and F. Florindo New Developments in the PuffinPlot Paleomagnetic Data Analysis Program, *Geochemistry Geophysics Geosystems*.

Sato, M., T. Terada, N. Mochizuki, and H. Tsunakawa (2019), Experimental Evaluation of Remanence Carriers Using the Microcoercivity-Unblocking Temperature Diagram, *Geochemistry Geophysics Geosystems*.

Vasquez, C. A., and Fazzito, S. Y., (2019). Simple hysteresis loop model for rock magnetic analysis, *Stud. Geophys. Geod.*, 64 (2020), DOI: 10.1007/s11200-019-1942-8 (in print).

Xuan, C., and H. Oda Sensor Response Estimate and Cross Calibration of Paleomagnetic Measurements on Pass-Through Superconducting Rock Magnetometers, *Geochemistry Geophysics Geosystems*.

Zhong, T., P. Liao, Q. X. Chen, N. Li, H. C. Deng, Q. J. Liu, Y. L. Luo, H. X. Lan, and C. Y. Li (2019), Imaging the Pore Structure in Geomaterials Using Rhodamine B Covalently Decorated Magnetic Nanoparticles, *Acs Earth and Space Chemistry*, 3(11), 2482-2489.

## Paleomagnetism

Ashwal, L. D. (2019), Wandering continents of the Indian Ocean, *South African Journal of Geology*, 122(4), 397-420.

Behar, N., R. Shaar, L. Tauxe, H. Asefaw, Y. Ebert, A. Heimann, A. A. P. Koppers, and H. G. Ron (2019), Paleomagnetism and Paleosecular Variations From the Plio-Pleistocene Golan Heights Volcanic Plateau, Israel, *Geochemistry Geophysics Geosystems*, 20(9), 4319-4335.

Derder, M. E. M., H. Djellit, B. Henry, S. Maouche, M. Amenna, R. Bestandji, H. Ymel, S. Gharbi, A. Abtout, and C. Dorbath Strong Neotectonic Block Rotations, Related to the Africa-Eurasia Convergence in Northern Algeria: Paleomagnetic Evidence From the Mitidja Basin, *Tectonics*.

Franceschinis, P. R., A. E. Rapalini, L. S. Bettucci, C. M. Dopico, and F. N. Milanese (2019), Paleomagnetic confirmation of the "unorthodox" configuration of Atlantica between 2.1 and 2.0 Ga, *Precambrian Research*, 334.

Fu, R. R., D. V. Kent, S. R. Hemming, P. Gutierrez, and J. R. Creveling

- (2020), Testing the occurrence of Late Jurassic true polar wander using the La Negra volcanics of northern Chile, *Earth and Planetary Science Letters*, 529.
- Gao, H. H., X. Q. Yang, J. P. Zhang, J. Peng, Q. X. Zhou, Y. Z. Weng, Q. Chen, G. H. Li, and N. Li (2019), Paleomagnetic records since similar to 80 ka from the southern South China Sea, *Chinese Journal of Geophysics-Chinese Edition*, 62(12), 4750-4765.
- Giorgis, S., E. Horsman, K. C. Burmeister, R. Rost, L. A. Herbert, A. Pivarunas, and M. Braunagel Constraints on Emplacement Rates of Intrusions in the Shallow Crust Based on Paleomagnetic Secular Variation, *Geophysical Research Letters*.
- Jones, L., and C. Verdel (2019), Animated reconstructions of the Late Cretaceous to Cenozoic northward migration of Australia, and implications for the generation of east Australian mafic magmatism: REPLY, *Geosphere*, 15(6), 2057-2061.
- Katagiri, T., H. Naruse, N. Ishikawa, and T. Hirata Collisional bending of the western Paleo-Kuril Arc deduced from paleomagnetic analysis and U-Pb age determination, *Island Arc*.
- Klootwijk, C. Paleomagnetism of the Carboniferous Gresford Block, Tamworth Belt, southern New England Orogen: minor counter-clockwise rotation of a primary arc segment, *Australian Journal of Earth Sciences*.
- Lerner, G. A., S. J. Cronin, G. M. Turner, and E. J. Piispa (2019), Recognizing long-runout pyroclastic flow deposits using paleomagnetism of ash, *Geological Society of America Bulletin*, 131(11-12), 1783-1793.
- Liu, J. X., X. F. Shi, Y. G. Liu, Q. S. Liu, Y. Liu, Q. Zhang, S. L. Ge, and J. H. Li A Thick Negative Polarity Anomaly in a Sediment Core From the Central Arctic Ocean: Geomagnetic Excursion Versus Reversal, *Journal of Geophysical Research-Solid Earth*.
- Musgrave, R. J., and P. W. Schmidt (2019), Animated reconstructions of the Late Cretaceous to Cenozoic northward migration of Australia, and implications for the generation of east Australian mafic magmatism: COMMENT, *Geosphere*, 15(6), 2053-2056.
- Perez-Rodriguez, N., J. Morales, M. N. Guilbaud, A. Goguitchaichvili, R. Cejudo-Ruiz, and M. D. Hernandez-Bernal (2020), Reassessment of the eruptive chronology of El Metate shield volcano (central-western Mexico) based on a comprehensive rock-magnetic, paleomagnetic and multi-approach paleointensity survey, *Quaternary Geochronology*, 55.
- Rowley, D. B. Reply to Comment on 'Comparing Paleomagnetic Study Means with Apparent Wander Paths: A Case Study and Paleomagnetic Test of the Greater India versus Greater Indian Basin Hypotheses', *Tectonics*.
- Ruh, J. B., L. Valero, L. Aghajari, E. Beamud, and G. Gharabeigli (2019), Vertical-axis rotation in East Kopet Dag, NE Iran, inferred from paleomagnetic data: oroclinal bending or complex local folding kinematics?, *Swiss Journal of Geosciences*, 112(2-3), 543-562.
- Speranza, F., A. G. Pellegrino, B. Zhang, R. Maniscalco, S. Y. Chen, and C. Hernandez-Moreno Paleomagnetic Evidence for 25-15 Ma Crust Fragmentation of North Indochina (23-26 degrees N): Consequence of Collision With Greater India NE Corner?, *Geochemistry Geophysics Geosystems*.
- Symons, D. T. A., and K. Kawasaki (2019), Jurassic location of the Yukon-Tanana terrane from palaeomagnetism of the folded Mississippian Tatlain batholith and Ragged stock, *Geophysical Journal International*, 219(3), 1660-1678.
- van Hinsbergen, D. J. J. Comment on "Comparing Paleomagnetic Study Means With Apparent Wander Paths: A Case Study and Paleomagnetic Test of the Greater India Versus Greater Indian Basin Hypotheses" by David B. Rowley, *Tectonics*.
- van Hinsbergen, L. P. P., D. J. J. van Hinsbergen, C. G. Langereis, M. J. Dekkers, B. Zanderink, and M. H. L. Deenen (2019), Triassic (Anisian and Rhaetian) palaeomagnetic poles from the Germanic Basin (Winterswijk, the Netherlands), *Journal of Palaeogeography-English*, 8.
- Westerweel, J., P. Roperch, A. Licht, G. Dupont-Nivet, Z. Win, F. Poblete, G. Ruffet, H. H. Swe, M. K. Thi, and D. W. Aung (2019), Burma Terrane part of the Trans-Tethyan arc during collision with India according to palaeomagnetic data (vol 12, pg 863, 2019), *Nature Geoscience*, 12(11), 959-959.
- Yan, Y. G., Q. Zhao, Y. P. Zhang, B. C. Huang, W. J. Zheng, and P. Z. Zhang Direct Paleomagnetic Constraint on the Closure of Paleotethys and Its Implications for Linking the Tibetan and Southeast Asian Blocks, *Geophysical Research Letters*.
- Yi, Z. Y., Y. Q. Liu, and J. G. Meert (2019), A true polar wander trigger for the Great Jurassic East Asian Aridification, *Geology*, 47(12), 1112-1116.
- Zhang, W. L., D. W. Zhang, X. M. Fang, T. Zhang, C. H. Chen, and M. D. Yan (2020), New paleomagnetic constraints on rift basin evolution in the northern Himalaya mountains, *Gondwana Research*, 77, 98-110.
- Zhao, J., B. C. Huang, and Y. G. Yan (2019), The Middle-Late Triassic Closure of the East Paleotethys Ocean: Paleomagnetic Evidence from the Baoshan Terrane, China, *Acta Geologica Sinica-English Edition*, 93(6), 1978-1979.
- Zhou, Y. N., X. Cheng, Y. Y. Wu, V. Kravchinsky, R. Q. Shao, W. J. Zhang, B. T. Wei, R. Y. Zhang, F. R. Lu, and H. N. Wu (2019), The northern Qiangtang Block rapid drift during the Triassic Period: Paleomagnetic evidence, *Geoscience Frontiers*, 10(6), 2313-2327.
- Zhou, Z. Z., et al. Palaeomagnetic assessment of tectonic rotation in Northeast Asia: implications for the coupling of intracontinental deformation and mantle convection, *International Geology Review*.
- Zhu, X., B. Wang, Y. Chen, and H. S. Liu Constraining the Intracontinental Tectonics of the SW Central Asian Orogenic Belt by the Early Permian Paleomagnetic Pole for the Turfan-Hami Block, *Journal of Geophysical Research-Solid Earth*.

## Note

The ISI Web of Science search used to compile the Current Articles section now includes Early Access articles, resulting in references lacking year and other publication details. In the future these will be filtered out.

## Summer School for Rock Magnetism at the IRM

June 1-10, 2020

The 10-day program is targeted at graduate students and advanced undergraduate students in rock magnetism, paleomagnetism, and associated fields. Students will receive intensive instruction in rock magnetic theory and laboratory techniques. A daily schedule of lectures, hands-on laboratory measurements, and data processing will introduce students to the fundamentals of rock magnetism and paleomagnetism and the practical aspects of collecting and interpreting data responsibly. Instructors for the summer school will be primarily IRM faculty and staff.

In addition to a \$100 registration fee, participants will be responsible for the costs of housing, meals, and travel to and from Minneapolis. For students from outside the Minneapolis-St. Paul area, housing will be available in University of Minnesota dormitories (~\$60 per night). A limited number of scholarships will be available to cover some of the costs for attending the summer program. Participation will be limited to 20 students, on a first-come first-served basis. Note that to foster academic diversity, a limit of 2 students per research group has been set; more students from the same institution will be considered if space allows. Applications and registration fees must be received by the deadline, April 30, 2020.

more details can be found at  
[www.irm.umn.edu](http://www.irm.umn.edu)

...Anisotropy, cont'd. from pg. 1

So shape anisotropy has been recognized for more than 4 centuries. Magnetocrystalline anisotropy was a much more recent discovery, dating to the middle of the 19th Century.



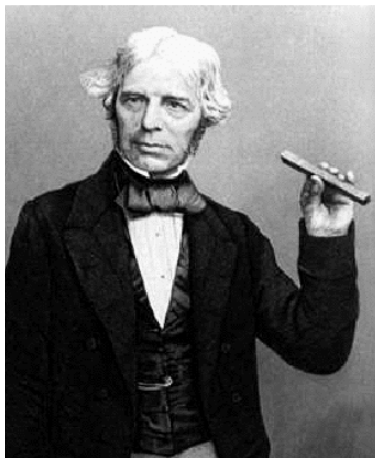
**Siméon-Denis Poisson**  
1781 - 1840

The possibility of an intrinsic structural anisotropy was described by Poisson in his *Mémoire sur la Théorie du Magnétisme* [1824]. His theory was based in part on the well-known observation that you can break or cut a bar magnet repeatedly and never obtain separate monopolar pieces; each piece always has a north and a south pole, and thus Poisson inferred that the magnetism must reside in microscopically small elements that act collectively to produce the magnetism of bulk matter. He allowed that these elements may be anisotropic, and arranged in such a way that the bulk material may be anisotropic, but he did not elaborate on the possibility because it had never

been observed: “Le rapport entre la somme des éléments magnétiques et le volume entier dans chaque corps aimanté n’est pas la seule donnée relative à ce corps, indépendamment de sa forme et de ses dimensions, d’où puisse dépendre l’intensité de ses actions magnétiques : la forme des éléments pourra aussi influencer sur cette intensité; et cette influence aura cela de particulier, qu’elle ne sera pas la même en des sens différens.” Here is a translated paraphrase from an excellent review paper by Kathleen Lonsdale [1938]: “... in crystalline matter the small ‘magnetic elements’ ... might be non-spherical and symmetrically arranged, and ... a finite spherical portion of such a substance would, when in the neighbourhood of a magnet, act differently according to the different orientations into which it might be turned.” So in effect Poisson predicted the possible existence of magnetocrystalline anisotropy, and within 25 years it was in fact discovered. And surprisingly, the effect was first observed in diamagnetic materials.

Two key steps toward that discovery were made by Michael Faraday. Faraday was deeply interested in the various forces of nature, how they interact with matter, and how they are related to one another. In 1831 he had made his discovery of electromagnetic induction, forming a new link between electricity and magnetism. And in Sept 1845 he was experimenting with magnetism and light, when he discovered that the polarization of light was affected when it was transmitted through a piece of glass, parallel to an applied magnetic field (Fig 3), by what is now known as the magneto-optic Faraday effect.

This was an important discovery in its own right, but it’s also part of the anisotropy story, because it triggered Faraday’s curiosity about the glass, which was nonmagnetic yet played a direct role in the magneto-optic effect, and he wondered whether it might also be affected more directly by magnetic forces. He obtained a stronger electromagnet and started a new series of experiments, and almost



**Michael Faraday**  
(1791-1867)

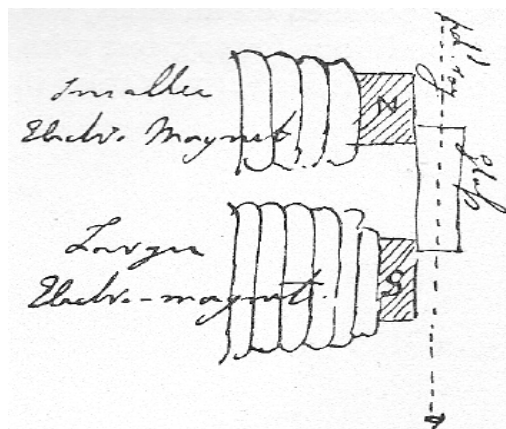


Fig. 3. Sketch from Faraday’s notebook, Sept 13, 1845, showing the experimental setup for his discovery of the magneto-optic effect. A smaller electromagnet (top) and a larger one (bottom) are arranged with opposite poles adjacent on the right. A ray of polarized light passes through a bar of leaded glass, along the magnetic lines of force, and the polarization is observed to rotate.

immediately he made his discovery of diamagnetism, on Nov 4, 1845. Fig 4 shows the experimental setup. He suspended a bar of heavy glass from a thread, so that it could rotate into whatever orientation it felt inclined to adopt between the poles of the strong electromagnet. He set the initial orientation by turning the thread, so that the long dimension was oblique to the magnet axis, and as soon as he activated the magnet, the bar rotated into an “equatorial” orientation, so that its long dimension was across the lines of force, rather than parallel to them as in the normal “axial” orientation adopted by magnetic materials. He interpreted this in terms of the ends of the bar moving from areas of strong magnetic force to areas of weaker force. This was his original operational definition of diamagnetism. As soon as the field was turned off, the bar rotated back to its initial orientation.

Now, as you can imagine, there are many factors that can affect the orientation and position adopted by a material in an applied magnetic field, including: the shapes of the pole pieces and the field uniformity; the shape of the sample; the susceptibility of the sample as well as any remanence it may have; the internal structure or intrinsic anisotropy

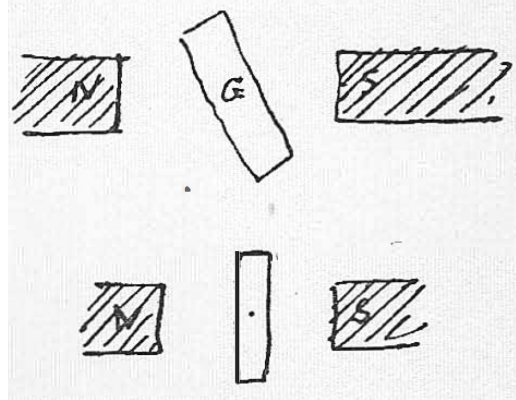


Fig. 4. Sketch from Faraday’s notebook, Nov 4, 1845, showing the experimental setup for his discovery of diamagnetism (plan view). The sample (G) is the same bar of heavy glass used in his magneto-optic discovery. Initially oriented obliquely to the magnetic axis (top), it rotated when the field was turned on, into an “equatorial” orientation with its long dimension perpendicular to the field (bottom)

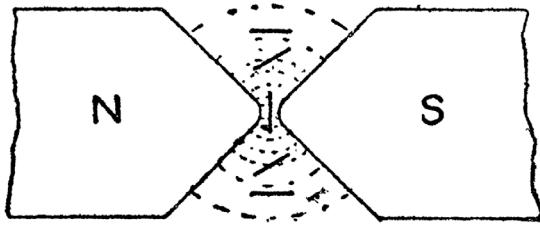


Figure 5. The orientation adopted by a sample when placed in different locations in a strongly non-uniform field [Bragg, 1927, based on experiments by John Tyndall in the 1840s].

of the sample, which Faraday named the “magnecrystalline force”; the sample homogeneity in terms of composition and crystallography; and the medium in which sample is immersed.

Figure 5 illustrates the complex behavior that can result from the superposition of these various effects. It comes from a review paper by William Bragg [1927], based on experiments carried out by John Tyndall in the 1840’s. The dashed curves show the magnetic lines of force between the tapered pole pieces, and the solid lines show the orientation adopted by a sample placed in various locations in the nonuniform field. The sample here is a piece of bread, pressed into a disk, and suspended from a thread as in Faraday’s experiment, and again we are looking down from above. When the sample is placed directly between the poles, it adopts the diamagnetic equatorial orientation with its long dimension across the lines of force. Here the field decays rapidly outward from the central axis, and the sample is able to occupy regions of lower magnetic force by orienting this way, so the principal factors controlling its orientation are its diamagnetic susceptibility and planar shape, combined with the strong field gradients. Farther from the axis, it rotates into an axial orientation, with its long dimension along the lines of force. Here the field gradients are lower, and the orientation is controlled by the sample anisotropy, related to its molecular structure and compressed state. Bragg is amused to note “It is quaint to observe how the bread, as it is moved ... to the poles, sets itself to pass neatly through the narrow gate and take up a parallel position on the further side”.

The discovery of diamagnetism excited great interest, and within a few years Faraday and his contemporaries had reached a clear understanding of the various factors involved in the magnetic alignment of samples, through careful experiments like this.

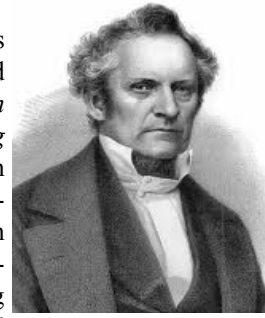
Two of those contemporaries who made important contributions were Julius Plücker and John Tyndall. In 1847 Plücker was actually the first to observe a clear effect of crystal structure in magnetic orientation experiments. In a review paper a decade later, he wrote: “In repeating Professor Faraday’s experiments, ... I was led to examine crystalline substances. Between the two poles of a strong electromagnet I first suspended a plate of tourmaline, then a plate of calcareous spar; and I remarked that these plates ... were acted upon in an extraordinary way, not dependent on their exterior shape, but solely on their crystalline structure.” [Plücker, 1858]. So here, finally, is the discovery of magnetocrystalline anisotropy, which had been predicted

by Poisson.

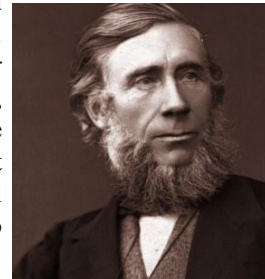
John Tyndall also carried out some key experiments and published numerous articles, which he collected and republished in 1870 in a book called *Researches on Diamagnetism and Magne-crystallic Action, Including the Question of Diamagnetic Polarity*. This question of diamagnetic polarity was a persistent point of disagreement between Tyndall and Faraday. Although they concurred on all of the experimental results collectively obtained, they did not agree on the underlying physical explanation for them. Tyndall was convinced that the proper explanation of diamagnetism necessarily involved induced diamagnetic poles, which formed with a polarity opposite that of normal magnets. Faraday was equally convinced that all of the observed phenomena could be explained in terms of the lines of force around and through the material, without any need for poles. Both carried out experiments attempting to prove or disprove the physical reality of diamagnetic poles, without conclusive result. I believe that this is quite probably the very beginning of the eternal debate about whether the  $B$  field or the  $H$  field is the fundamental magnetic field (see *IRM Quarterly* v. 24 n. 4 and also v. 18 n. 1). But that’s another story.

As we move into the 20th Century, we find an increasing interest in the magnetic anisotropy of bulk natural materials (rocks and sediments), and its geological significance. In 1929, Johann Koenigsberger published a remarkable paper with the simple title “*Method for measuring the susceptibility of rocks.*” His method was adapted from Kelvin’s mathematical method of images in electrostatics.

Figure 6 illustrates Koenigsberger’s design and the method of images. Suppose we have a half-space, filled with a uniform material having a particular dielectric constant (or magnetic susceptibility), bounded below by a planar surface that separates it from vacuum or air. If



Julius Plücker (1801-1868)



John Tyndall (1820-1893)

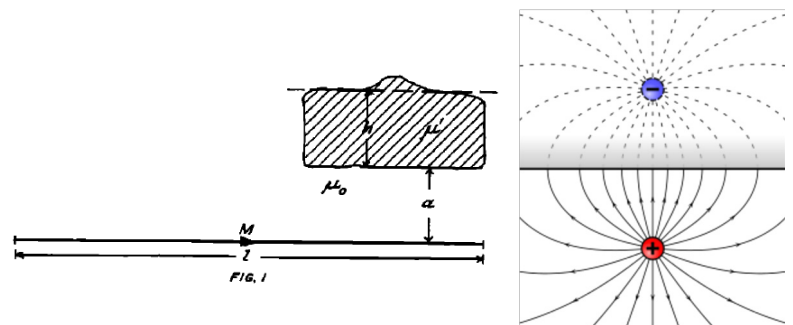


Fig. 6. (left) Koenigsberger’s [1929] drawing of his instrumental approach: a magnetic needle  $M$ , of length  $l$ , effectively has an isolated pole at its tip, which interacts with a sample having thickness  $h$  and permeability  $\mu$ , and an attractive force acts across the distance  $a$  according to the image affect. (right) sketch of the electrostatic image effect from Wikipedia; see text for description.

we introduce a point charge or a magnetic pole into the lower space, it affects the upper material, polarizing or magnetizing it, and the effect is equivalent to placing an imaginary charge or pole symmetrically in the upper material (a mirror image), with a strength that depends on the material properties. The great advantage of this method is that it provides a direct way to calculate the mutual force



**Johann Georg Koenigsberger (1874-1946)**

acting between the discrete pole or charge and the distributed volume of material.

Koenigsberger's approach to measuring susceptibility is remarkably simple. The instrument consists primarily of a long magnetic needle, which effectively has an isolated pole at the end. When a sample having a planar surface is placed near the end of the needle, an induced magnetization is produced in the sample, and that in turn exerts a force on the pole by the image effect. Deflection of the magnetic needle is proportional to this force and therefore gives an indication of the susceptibility of the sample. Due to the simplicity of the instrumentation, "The method is

suitable for use in the field with a variometer to determine the susceptibility of samples of rocks".

When the sample has a remanent moment, that also contributes to the deflection, but Koenigsberger recognized that he could simply rotate the sample by 180° to change the sign of that contribution, and thus obtain both the induced intensity and the parallel component of remanence, giving the famous Koenigsberger ratio. But more to the point for this discussion, he was also able to measure the anisotropy of magnetic susceptibility on suitably shaped samples, in the field, with a resolution down to about 5%. He notes that "Observations on about a hundred samples have shown that massive igneous rocks have normally... magnetic isotropy but that crystalline schists often possess a large magnetic anisotropy. The anisotropy  $K_{\text{parallel}}/K_{\text{perpendicular}}$  ranges from 1.05 to 2." Remarkably, he then offers two possible physical mechanisms for the observed anisotropy: "This may be explained by assuming an anisometric distribution of magnetic isotropic minerals or also of anisotropic minerals which have a quite irregular arrangement with respect to their crystallographic orientation." In other words, the directional dependence may be due to distribution anisotropy (as later proposed by Mike Fuller [1961] and by Rob Hargraves [1991]), or it may be a consequence of the statistical preferred orientations of crystals having magnetocrystalline and/or shape anisotropies (as in the models of Owens [1974] and Hrouda [1987]), with imperfect alignment of the crystals resulting in a bulk anisotropy that may be significantly less than that of the individual crystals.

Gustav Ising is often mentioned as one of the pioneers of magnetic anisotropy research (e.g., Parés [2015]; see also Ted Evans' 2017 article in the IRM Quarterly). In his most relevant work, *On the magnetic properties of varved clay* [1942] he begins with a surprising initial hypothesis: "...being very skeptical as regards the constancy of remanent magnetic moments in general, I thought it conceivable that the varved clay, during its sedimentation, might have acquired an anisotropy of susceptibility which had thence remained as an invariable quality of material, independent of possible changes in its remanent moment."



**Gustav Ising (1883-1960)**

In other words, he thought that AMS might possibly be a more reliable indicator of paleofield orientation than the NRM is. Stepwise cleaning was as yet unknown, so NRM orientations could very well be compromised. Further it seemed conceivable that the depositional magnetic field could exert enough direct control of particle long-axis orientations to produce an AMS signature.

What he found instead was a dominantly gravitational fabric: "The large excess of susceptibility of the strata-plane (about 10%) constituting a kind of magnetic schist structure that almost conceals the azimuthal anisotropy, must certainly be ascribed not to magnetic field actions, but to forces of purely mechanical origin during and after the sedimentation process; even after settling...an additional levelling may have been caused by the pressure of the overlying clay." He also observed that the NRM inclinations were systematically shallower than expected.

He still hoped that the AMS lineation might reflect the paleofield declination, but "The instrumental sensitivity ... has not yet been quite sufficient to determine accurately the azimuthal direction in the strata-plane of the axis of maximal susceptibility, which seems to be decisive for the problem of determining the secular variation of the declination from clay measurements." Although Ising's approach has not proven to be suitable for determining paleofield orientations, I have a particular interest in it, as it provided the basis for my postdoctoral work with Subir Banerjee before the inception of the IRM, looking at the relationship between sedimentary remanence and the anisotropy of partial anhysteretic remanence. Ted Evans also describes Ising's pioneering studies in environmental magnetism, and notes that Ising played a role in the invention of the particle accelerator.

John Graham is well known in paleomagnetism as the originator of the fold test and the conglomerate test for paleomagnetic stability [Graham, 1949]. He also published a GSA abstract in 1954 with the title "Magnetic susceptibility anisotropy, an unexploited petrofabric element", which is frequently mentioned as one of the pioneering works of magnetic fabric analysis. Twelve years later he provided a detailed look at sedimentary rocks of the Appalachians that have undergone various degrees of deformation [Graham, 1966]. Before this there had been several anisotropy papers concerned mainly with paleomagnetic fidelity (e.g., Hargraves [1959], Stacey [1960], Fuller [1960]), but this is the first paper I am aware of in which the structural applications of AMS were the primary emphasis.

Figure 7 shows his generalization of his results into an evolutionary diagram of the magnetic fabric with increasing deformation. The undeformed sedimentary fabric is mostly planar with a vertical minimum axis. Initial deformation reorients the ellipsoid so that the intermediate axis aligns with the horizontal compression axis. Continued compression leads to systematic changes in the ellipsoid shape. The third stage has a purely linear fabric ( $V=0^\circ$ ), with the vertical tectonic foliation superimposed on the horizontal sedimentary foliation to produce an intersection lineation. Then we go through another triaxial state, followed by a purely oblate ellipsoid ( $V=90^\circ$ ) as the tec-

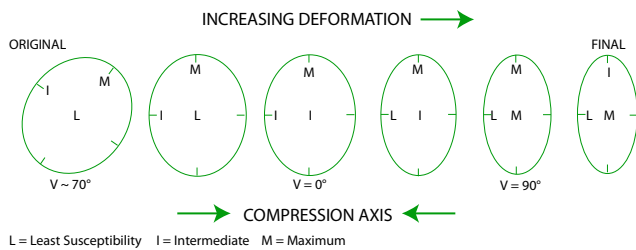


Figure 7. Evolution of sedimentary magnetic fabric with increasing deformation, redrawn from Graham [1966].

tonic foliation becomes dominant. Finally for strongly deformed rocks with vertical extension, the vertical axis becomes the unique maximum axis of a triaxial ellipsoid. Various modified versions of this figure are still widely used in the structural anisotropy literature.

The deep and rich history of magnetic anisotropy research includes numerous other people and ideas that are worthy of discussion, but due to the limitations of space and time, we will reserve them for future articles.

## References and Additional Reading

Bragg, W. (1927), Tyndall's Experiments on Magne-Crystallic Action, *The Scientific Monthly*, 25(1), 65-79

Bragg, W. H. (1931), Michael Faraday, *The Scientific Monthly*, 33(6), 481-499

Doell, R. R. (1972), Memorial to John Warren Graham, 1918—1971, *Geological Society of America Memorials*, 3, 105-108

Evans, M. E. (2017), Gustaf Ising's Early Work on Magnetic Fabrics, *IRM Quarterly* v. 27, n. 1.

Faraday, M. (1846), On new magnetic actions, and on the magnetic condition of all matter, *Journal of the Franklin Institute*, 42(1), 66-69, doi: [https://doi.org/10.1016/0016-0032\(46\)90194-9](https://doi.org/10.1016/0016-0032(46)90194-9).

Faraday, M. (1932), *Faraday's diary, being the various philosophical notes of experimental investigation made by Michael Faraday, during the years 1820-1862 and bequeathed by him to the Royal institution of Great Britain*, v., London: G. Bell and sons, ltd., London.

Fuller, M. D. (1960), Anisotropy of Susceptibility and the Natural Remanent Magnetization of Some Welsh Slates, *Nature*, 186(4727), 791-792, doi: 10.1038/186791a0.

Fuller, M. (1961), *Magnetic Anisotropy of Rocks*, Ph.D. thesis, Cambridge University.

Gilbert, W. (1600), *De magnete, magneticisque corporibus et de magno magnete tellure*, second edition ed., v., Petrus Short, London. translation by Silvanus Phillips Thompson and the Gilbert Club (1900). London: Chiswick Press.

Graham, J. W. (1949), The stability and significance of magnetism in sedimentary rocks, *J. Geophys. Res.*, 54, 131-167

Graham, J. W. (1954), Magnetic susceptibility anisotropy, an unexploited petrofabric element, *Geol. Soc. Am. Bull.*, 65, 1257-1258

Graham, J. W. (1966), Significance of magnetic anisotropy in Appalachian sedimentary rocks, in *The Earth Beneath the Continents*, edited by J. S. Steinhart and T. J. Smith, vol. 10, pp. 627-648, American Geophysical Union, Geophysical Monograph Series, Washington.

Hargraves, R. B. (1959), Magnetic anisotropy and remanent magnetism in hemo-ilmenite from ore deposits at Allard Lake, Quebec, *J. Geophys. Res.*, 64, 1565-1578

Hargraves, R. B., D. Johnson, and C. Y. Chan (1991), Distribu-

tion anisotropy: the cause of AMS in igneous rocks?, *Geophys. Res. Lett.*, 18, 2193-2196

Hrouda, F. (1987), Mathematical model relationship between the paramagnetic anisotropy and strain in slates, *Tectonophys.*, 142, 323-327

Ising, G. (1942), On the magnetic properties of varved clay, *Arkiv for Matematik, Astronomi och Fysik*, 29A, 1-37

Jackson, M. (2008), *This Thing Called Flux* (a primer), *IRM Quarterly* v. 18, n. 1.

Jackson, R. (2015), John Tyndall and the Early History of Diamagnetism, *Annals of Science*, 72(4), 435-489, doi: 10.1080/00033790.2014.929743.

Koenigsberger, J. G. (1929), Method for measuring the susceptibility of rocks, *Terr. Magn. Atmos. Electr.*, 34(3), 209-214, doi: 10.1029/TE034i003p00209.

Lonsdale, K. (1937), Diamagnetic and paramagnetic anisotropy of crystals, *Rep. Prog. Phys.*, 4(1), 368-389, doi: 10.1088/0034-4885/4/1/325.

Nye, J. F. (1957), *Physical Properties of Crystals*, 322 pp., Oxford University Press, London.

Owens, W. H. (1974), Mathematical model studies on factors affecting the magnetic anisotropy of deformed rocks, *Tectonophys.*, 24, 115-131

Parés, J. M. (2015), Sixty years of anisotropy of magnetic susceptibility in deformed sedimentary rocks, *Frontiers in Earth Science*, 3(4), doi: 10.3389/feart.2015.00004.

Plücker, J. (1858), On the Magnetic Induction of Crystals, *Philosophical Transactions of the Royal Society of London*, 148, 543-587

Poisson, S.-D. (1824), *Mémoire sur la théorie du magnétisme*, 92 pp., Impr. royale, Paris.

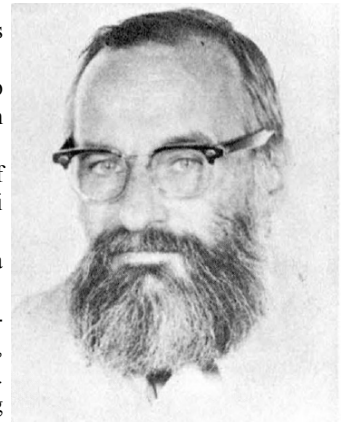
Stacey, F. D. (1960), Magnetic anisotropy of igneous rock, *J. Geophys. Res.*, 65, 2429-2442

Stacey, F. D., B. Moskowitz, M. Jackson, D. J. Dunlop, Ö. Özdemir, S. K. Banerjee (2014), A new basis for the SI system of units: occasion to reconsider the presentation and teaching of magnetism, *IRM Quarterly* v. 24, n. 4.

Thompson, W., and C. Sabine (1851), X. A mathematical theory of magnetism, *Philosophical Transactions of the Royal Society of London*, 141, 243-268, doi: doi:10.1098/rstl.1851.0012.

Tyndall, J. (1870), *Researches on diamagnetism and magne-crystallic action, including the question of diamagnetic polarity*, v., xix, 361 pp., Longmans, Green, and co., London.

Tyndall, J., and H. Knoblauch (1850), XXIV. On the deportment of crystalline bodies between the poles of a magnet, *The London, Edinburgh, and Dublin Philosophical Magazine and Journal of Science*, 36(242), 178-183, doi: 10.1080/14786445008646457.



John W. Graham (1918-1971)

**Correction:** Since distributing the IRMQ29-3 it was brought to my attention that I had omitted to cite the article by Smirnov (2009) on the effect of grain size on the FC/ZFC ratio (the  $R_{LT}$  ratio). Smirnov (2009) reported  $R_{LT}$  values of 1.12 for synthetic magnetite with the smallest mean grain size of 150 nm (range 30-600 nm), effectively demonstrating SD-like behavior in grain size ranges that are actually dominated by MD particles. I have since modified the article to include these observations and the updated article is posted on the IRM website. Dario Bilardello

University of Minnesota  
John T. Tate Hall, Room 150  
116 Church Street SE  
Minneapolis, MN 55455-0149  
phone: (612) 624-5274  
e-mail: irm@umn.edu  
www.irm.umn.edu

Nonprofit Org.  
U.S Postage  
PAID  
Twin Cities, MN  
Permit No. 90155

# The IRM Quarterly

The *Institute for Rock Magnetism* is dedicated to providing state-of-the-art facilities and technical expertise free of charge to any interested researcher who applies and is accepted as a Visiting Fellow. Short proposals are accepted semi-annually in spring and fall for work to be done in a 10-day period during the following half year. Shorter, less formal visits are arranged on an individual basis through the Facilities Manager.

The *IRM* staff consists of **Subir Banerjee**, Professor/Founding Director; **Bruce Moskowitz**, Professor/Director; **Joshua Feinberg**, Assistant Professor/Associate Director; **Mike Jackson**, **Peat Solheid** and **Dario Bilardello**, Staff Scientists.

Funding for the *IRM* is provided by the **National Science Foundation**, the **W. M. Keck Foundation**, and the **University of Minnesota**.

The *IRM Quarterly* is published four times a year by the staff of the *IRM*. If you or someone you know would like to be on our mailing list, if you have something you would like to contribute (e.g., titles plus abstracts of papers in press), or if you have any suggestions to improve the newsletter, please notify the editor:

**Dario Bilardello**  
Institute for Rock Magnetism  
University of Minnesota  
John T. Tate Hall, Room 150  
116 Church Street SE  
Minneapolis, MN 55455-0149  
phone: (612) 624-5274  
e-mail: irm@umn.edu  
www.irm.umn.edu

The U of M is committed to the policy that all people shall have equal access to its programs, facilities, and employment without regard to race, religion, color, sex, national origin, handicap, age, veteran status, or sexual orientation.

The next Visiting Fellowship  
application deadline is  
April 30, 2013.

The IRM is pleased to welcome  
new Facility Manager  
Maxwell Brown



UNIVERSITY OF MINNESOTA